# Cooling crystallization under influence of a strong DC electric field

## A novel way to produce specific polymorphs

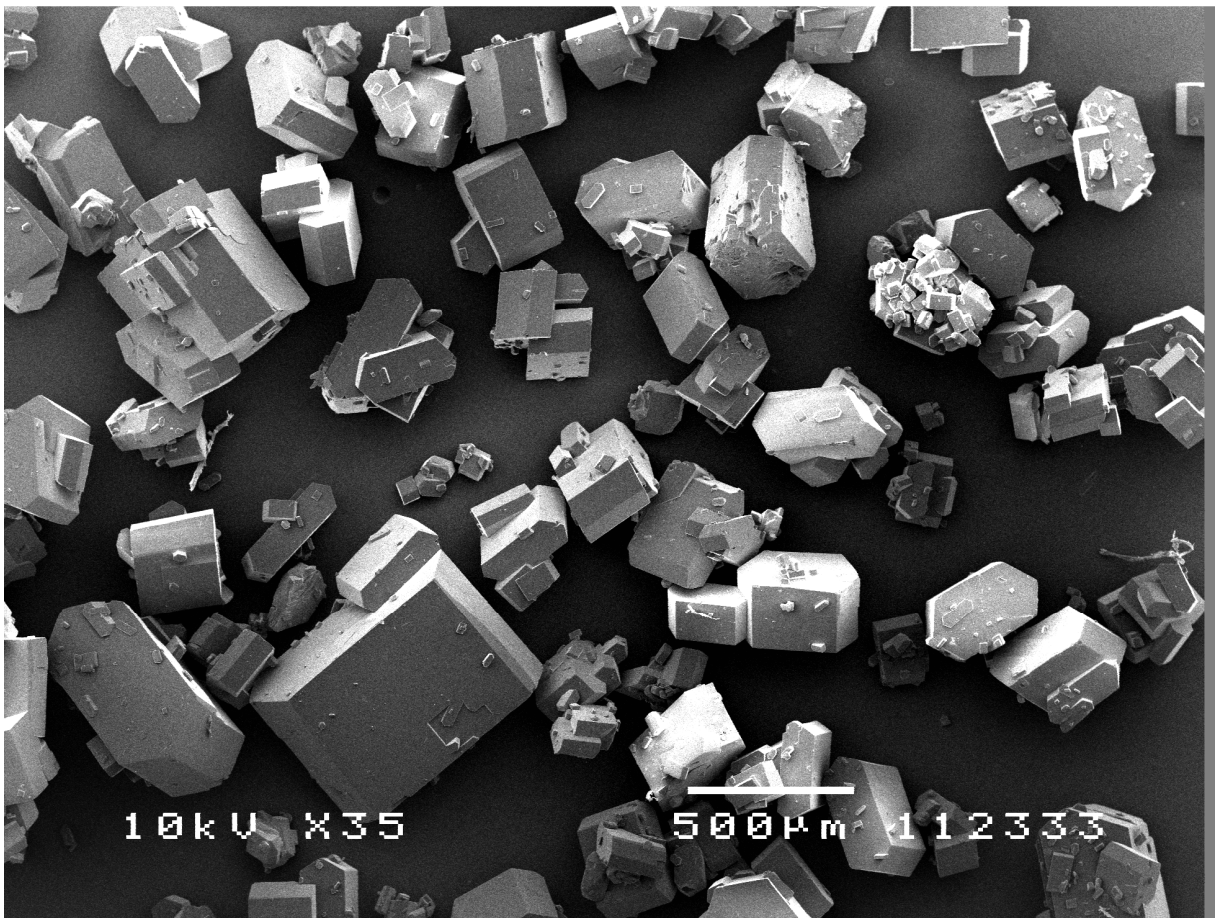



| | |
|---|---|
| Name | Nick Wursten |
| Student number | 1256319 |
| Master program | Chemical Engineering |
| | Delft University of Technology |
| Research group | Intensified Reaction & Separation Systems |

Exam Committee

| | |
|---|---|
| 1st supervisor | Dr. Ir. J.H. Ter Horst |
| 2nd supervisor | Prof. Dr. Ir. A.I. Stankiewicz |
| 3rd supervisor | Prof. Dr. Ir. A. Schmidt-Ott |


| | |
|---|---|
| Start date | 01-07-2011 |
| End date | 21-08-2012 |

# Cooling crystallization under influence of a strong DC electric field

## A novel way to produce specific polymorphs

**Delft University of Technology**
Faculty of Applied Sciences
Process and Energy Department
Intensified Reaction & Separation Systems

**Master of Science Thesis**
Nick Wursten
Chemical Engineering
1256319
nick_wursten@hotmail.com

**Supervisor**
Norbert Radacsi

*April 2012*

**Exam Committee**
Dr. Ir. J.H. ter Horst
Prof. Dr. Ir. A.I. Stankiewicz
Prof. Dr. A. Schmidt-Ott

# Abstract

Polymorphism is the ability of solid material to exist in more than one form or crystal structure. It is especially important for the pharmaceutical industry, where often one particular polymorph is wanted. Polymorphic formation is primarily determined by nucleation and crystal growth, which are governed by thermodynamics, kinetics, and fluid dynamics. Due to all these influences it is hard to control the polymorphic outcome of a crystallization process.

This research investigated the effect of a strong DC electric field on crystal nucleation and the polymorphic outcome of a cooling crystallization process. In principle, the electric field could have three effects on crystal nucleation: alignment of molecules, change in nucleation work, and inducing concentration gradients. The materials were chosen so that these effects were taken into account. A low dielectric constant and dipole moment are favored for the solvent, whereas for the crystalline phase a high dipole moment and distinct morphology are preferred.

Two experimental setups were built to study these effects. The Crystalline setup with an on-board Raman spectrometer was used for *in situ* investigation of the applied DC electric field effect on nucleation and polymorphic transition. This setup offers a controlled way of cooling crystallization under influence of an inhomogeneous electric field. The parallel-plate setup consisted of a glass cuvette with mounted electrodes on the inside walls, which provided a system where the polymorphic outcome can be studied under influence of a homogeneous electric field.

Two model compounds (isonicotinamide and 4-hydroxybenzoic acid) were examined in the absence and presence of an electric field with Raman spectroscopy and XRPD. These analytical techniques confirmed that a constant electric field ($\pm 10^5$ V $m^{-1}$) during crystallization affected the polymorphic outcome. In the case of isonicotinamide it was observed that the purely metastable form I is obtained in the absence of the electric field and that a mixture of the stable form II and metastable form I is obtained in the presence of the electric field. For 4-hydroxybenzoic acid a mixture of both polymorphs was produced in the absence of an electric field, while the metastable polymorph was acquired in the presence of an electric field. Thus, the electric field has a significant influence on nucleation and the polymorphic outcome of a crystallization process. In future research this results could, for instance, be used in the pharmaceutical industry in order to control the polymorphic outcome of a cooling crystallization process.

# Table of content

# 1. Introduction

Nowadays, polymorphism plays an important role in the fields of pharmaceuticals, foods, agrochemicals, and explosives. Especially for the pharmaceutical industry, where polymorphism is widespread among numerous compounds, it is of vital importance. Polymorphism is the ability of a solid material to exist in more than one form or crystal structure. A distinction is made between two types of polymorphism based on structural formation. Packing polymorphism results from a difference in crystal packing arrangement, while conformational polymorphism is the result of the existence of different conformers of the same molecule. Due to these differences in crystal packing and/or molecular conformation, polymorphs exhibit different physical properties (e.g. solubility, density, melting point, and morphology). Polymorphic formation is primarily determined by nucleation and crystal growth, which are governed by thermodynamics, kinetics, and fluid dynamics. From a thermodynamic point of view crystallization must result in an overall decrease of the Gibbs free energy, whereby often the stable polymorph is formed. The drive to a minimum in energy is, however, balanced by the kinetic tendency of the system to crystallize as fast as possible to relieve the supersaturation. Thus polymorphic formation in a crystallization process is the result of a trade-off between kinetics and thermodynamics.[1]

In spite of the benefits there are considerable practical difficulties that can arise by polymorphism such as the reproducibility of a specific polymorph and preventing its transformation to an undesirable form.[2] Such problems may lead to serious consequences of which the Ritonavir case is famous. Ritonavir is an important pharmaceutical compound that prevents HIV to develop into AIDS by inhibiting particular proteins. Two years after the market introduction it turned out that a previously unknown and more stable polymorph appeared in the product. The problem was that the solubility of this new polymorph was much lower and so upon administering Ritonavir the concentration in the body drastically dropped to a level, where the pharmaceutical was not active anymore. Due to this effect pharmaceutical supplier Abbott had to take Ritonavir of the market.[3] This example marks the practical importance and consequences of polymorphism and shows that polymorphic control is important, but sometimes difficult to achieve. Research focused on the electric field effect on crystallization processes (e.g. nucleation), which hopefully could be used towards polymorphic control.

From theory and previous research it is known that an electric field could have several effects on the crystallization process. It could influence the nucleation work[4][5], nucleation kinetics[6], and local supersaturation[7]. Hammadi and Veesler recently reviewed important research topics in protein crystallization under influence of an electric field. Both internal and external application of Direct Current and Alternating Current were discussed.[8] Moreno et al. stated that control of lysosome nucleation was accomplished in the presence of an internal electric field.[9] Previous research by Nogueira et al. reported that the crystal structure of a second harmonic generation compound changed when recrystallizing it under influence of an electric field.[10] The main goal of this research was to investigate and understand the effect of a strong DC electric field on crystal nucleation and polymorphic outcome in a cooling crystallization process. The outcome of this research could find its application in the pharmaceutical industry and could be used to control polymorphism.

# 2. Theoretical background

*In this chapter the theoretical background of polymorphism and crystallization under the influence of an electric field is given. The first paragraph 2.1 describes what polymorphism is and why it is important. Also the crystallization parameters, which have an influence on the polymorphic outcome are discussed. Section 2.2 reviews the three main effects of an electric field on the crystallization process. Appendix A describes conventional nucleation and appendix B gives a brief explanation of the basic physics used.*

## 2.1 Polymorphism

Polymorphism is the ability of a solid material to exist in more than one form or crystal structure. A polymorph is defined as a solid crystalline phase of a given compound resulting from the possibility of at least two crystalline arrangements of the molecules of that compound in the solid state.[11] Compounds can also crystallize in different forms containing solvent molecules incorporated within the crystal structure, which are called solvates (or in the case of water hydrates). This phenomenon is referred to as pseudo-polymorphism. Polymorphism is important, because different polymorphs usually exhibit different physical properties (e.g. solubility, morphology, and bioavailability). For instance, paracetamol has two common polymorphs at ambient conditions. The monoclinic structure is stable and forms readily, but it cannot be compressed into tablets due to poor compressibility. The orthorhombic structure is a metastable form, which requires other conditions to produce, but it is easier to press into tablets. This example marks the practical importance of polymorphism, but in spite of the benefits there are considerable (practical) difficulties that can arise. For example, the reproducibility of a specific polymorph and preventing its transformation to an undesirable form during the lifetime of its application.[1][2]

The crystal structure with the lowest free energy at given conditions is the stable polymorph, while all other structures (which have higher free energies) are the metastable forms. When a metastable state is in equilibrium, it is susceptible to fall into a lower-energy state by only a minor interaction. This means that the metastable polymorph has a thermodynamic tendency to transform into a more stable form, which can be achieved by either solvent-mediated transformation or, less likely, via a solid-state transformation.[1][12] In terms of thermodynamics with regard to polymorphic transformations, two types are distinguished, namely monotropic and enantiotropic transformations. A monotropic transformation is an irreversible transition from one polymorph to another. Enantiotropic transformation shows a crossing point before the various melting points, which means that it is possible to convert reversibly between the two polymorphs upon heating and cooling.[2][3] Figure 1 depicts a monotropic as well as an enantiotropic system.

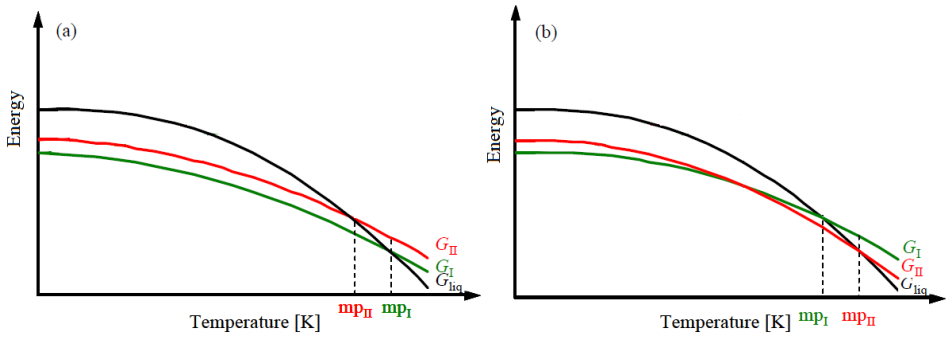


**Figure 1: (a) Monotropic irreversible system; Red and Green line do not cross each other (b) Enantiotropic reversible system; Red and Green line cross each other at the transition point.**

Polymorphic formation is primarily determined by nucleation and crystal growth, which are governed by thermodynamics, kinetics, and fluid dynamics. In a polymorphic system a compound can crystallize in a number of structures all of which have different free energies. Thermodynamically, crystallization tends to minimize the systems free energy, which often leads to the formation of the stable polymorph. The drive to a minimum in energy is, however, often balanced by the kinetic tendency of the system to crystallize as fast as possible to relieve the supersaturation. Thus, if the metastable polymorph crystallizes more readily than the stable form, it will appear as first in the system. According to Ostwald's rule it is generally not the most stable, but the least stable polymorph that crystallizes first. So polymorphic formation in a crystallization process is the result of a trade-off between kinetics and thermodynamics.[1]

Fluid dynamics also plays an important role in the polymorphic formation, because it often determines the local supersaturation in a crystallization process. Primary nucleation (which highly depends on supersaturation) is the decisive step in the determination of the polymorphic form during a crystallization process. So variations of supersaturation in space and time strongly influences the polymorphic outcome. Thus to control polymorphism, the dynamics should be controlled as well.

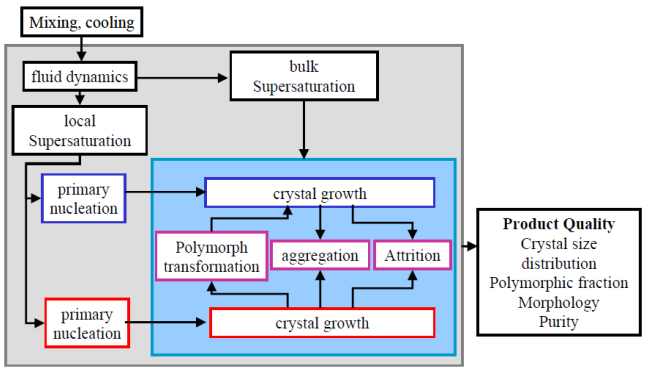


**Figure 2: Roles of thermodynamics, kinetics, and fluid dynamics in a crystallization process.**

Figure 2 shows the important role of thermodynamics, kinetics, and fluid dynamics in a crystallization process. Thermodynamics determines the stable and metastable polymorphs and their intrinsic properties such as solubility. The most common way to depict this is by a solubility curve, which gives the temperature dependence of the solubility of a compound in a solvent. From this it can be determined what process conditions (e.g. temperature and supersaturation) are necessary to obtain a particular polymorph. Fluid dynamics determines the local supersaturation, which strongly governs

the primary nucleation in a crystallization process. Because the nucleation rate and crystal growth rate are all dependent on supersaturation, the stable and metastable forms have different nucleation and crystal growth rates. So which form will first appear is kinetically determined by the competitive nucleation and growth rates of the different polymorphic forms.

Besides supersaturation, there are other factors that can also influence the result of the polymorphic outcome. According to Kitamura et al. these factors can be divided into primary and secondary factors. Primary factors are supersaturation, temperature, stirring rate, and mixing rate of reactant solutions. Choice of solvent, additives, seed, and pH are considered to be secondary factors.[1][2][13]

## 2.2 Crystallization

### 2.2.1 Supersaturation

Crystallization is defined as the formation of a solid crystalline phase from a fluid. To provoke crystallization the thermodynamic state of a solution is shifted away from the conditions of phase equilibrium by an external action. The driving force for any crystallization process is supersaturation, which is a thermodynamically unstable state were more solute is dissolved in the solution than the maximum solubility. Supersaturation can be accomplished by changing the solubility of the solute in the solution or by selective removal of the solvent. The first can be achieved in several ways, but temperature reduction and changing the composition of the solvent are most commonly used. They are called cooling and anti-solvent crystallization, respectively. Solvent removal is usually done by evaporation, which is known as evaporative crystallization. Supersaturation is an important parameter in the crystallization process, because it determines the mechanism and rate of the elementary processes such as nucleation and crystal growth. It can be expressed in terms of the supersaturation ratio, which depends on the actual concentration $c$ and the equilibrium concentration $c^*$ (solubility).[12]

$$S = \frac{c}{c^*} \tag{2-1}$$

It should be noticed that the actual thermodynamic driving force is the difference in chemical potential between the solution and the crystalline phase.

$$\Delta\mu = \mu_s - \mu_c = RT \ln \frac{\gamma_a c}{\gamma_a^* c^*} \tag{2-2}$$

This chemical potential difference is only equivalent to supersaturation when the deviation from an ideal solution is negligible and supersaturation is relatively small. At relatively low supersaturation the activity coefficients are nearly equal. With these assumptions equation 2-2 simplifies to

$$\frac{\Delta\mu}{RT} \approx S - 1 = \sigma \tag{2-3}$$

For processes performed at constant temperature and pressure at low supersaturation, the thermodynamically exact supersaturation is approximated by the practical quantity $\sigma$, which is called the relative supersaturation.[14][15][16]

### 2.2.2 Electric field effects on crystallization

In this thesis it is of great importance to understand the effects of an electric field on the different crystallization processes. Crystallization consists of several processes knowing nucleation, crystal growth and agglomeration. From theory and previous research it is known that an electric field has several effects on the crystallization process. It could influence the nucleation work[4][5], nucleation kinetics[6], and local supersaturation.[8]

#### 2.2.2.1 Nucleation work

Because nucleation is the crucial step in the polymorphic outcome, it is essential to know the influence of an electric field on this process. Two different mechanisms are known for crystal nucleation namely primary and secondary nucleation (attrition). In this research focus is on primary nucleation, which is the crystal creation within a supersaturated solution. Primary nucleation is divided into homogeneous and heterogeneous nucleation. The formation of crystals from a clear supersaturated solution is known as homogeneous nucleation, while heterogeneous nucleation is known as the formation of crystals on foreign substances (e.g. seeds, reactor wall, dust).

Nucleation is a two-step process where first the formation of small clusters of solute molecules takes place followed by an organizational step in which the cluster takes on a crystalline structure. To understand the effect of an electric field on nucleation consider a spherical liquid drop within a system where an electric field is present in the space between two parallel metallic plates of relatively large surface area. The Gibbs free energy required for the formation of a crystalline cluster in this drop (kept at constant supersaturation) is given by

$$\Delta G = 4\pi r^2 \gamma - x k_B T \ln(S) + \Delta G_E \qquad \textbf{(2-4)}$$

where $r$ is the sphere radius and $\gamma$ is the interfacial tension. The first and second term represent the surface- and volume energy, respectively, in the classical nucleation theory. The third term accounts for the change in electrostatic energy when $x$ molecules transform into a cluster in the presence of an electric field. An expression for the electric field contribution to nucleation work was derived by Kashchiev[4]

$$\Delta G_E = -x k_B T \psi E^2 \qquad \textbf{(2-5)}$$

where $x$ is the number of molecules in the cluster, $E$ is the electric field strength, and ψ is a constant in which the term $(1 - \varepsilon_c/\varepsilon_S)$ appears (where $\varepsilon_c$ and $\varepsilon_S$ are the dielectric constants of the crystalline phase and solution, respectively). Nucleation work may either be reduced (for $\varepsilon_c < \varepsilon_S$) or enhanced (for $\varepsilon_c > \varepsilon_S$) by the electric field.[4][5][8]

To determine the radius of the critical nucleus the total $\Delta G$ must be minimized with respect to $r$. The critical radius $r^*$ is given by equation 2-6.

$$r^* = \frac{2\gamma\omega}{k_B T\left(\ln S + \psi E^2\right)} \qquad \textbf{(2-6)}$$

So its size depends on supersaturation, interfacial energy, and the electric field strength. Clusters with radii exceeding the critical nucleus are stable and have the tendency to grow to macroscopic

size. The Gibbs free energy needed to create a nucleus can be determined by combining equations 2-4 and 2-6

$$\Delta G^* = \frac{16\pi\ \gamma^3 \omega^2}{3\left[k_B T\left(\ln S + \psi E^2\right)\right]^2} \qquad \textbf{(2-7)}$$

where $\omega$ is the molecular volume and $\Delta G^*$ is the nucleation work. Thus the change in free energy will depend on the magnitude of the field strength and supersaturation. Homogeneous nucleation can only occur if this energy barrier is overcome. The time it takes for homogeneous nucleation to happen is called the induction time. It is defined as the period of time between the achievement of supersaturation and the detection of crystals. With increasing supersaturation and field strength, the energy barrier is decreased. So as a result the induction time decreases with increasing supersaturation or electric field strength. From equation 2-7 the nucleation rate $J$ can be obtained

$$J = A\exp\left(-\frac{\Delta G^*}{k_B T}\right) \qquad \textbf{(2-8)}$$

where $A$ is a pre-exponential factor. The nucleation rate for homogeneous nucleation is expressed in number of nuclei per unit of volume per unit of time.[3][5]

Heterogeneous nucleation happens in the presence of foreign substances, because a phase boundary or impurity lowers the free energy needed to reach the critical nucleus size. The reason for this is that the activation energy for nucleation work is lowered when nuclei form on preexisting surfaces or interfaces, since the surface tension is reduced. In other words, it is easier for nucleation to occur at surfaces and interfaces than from solution. Therefore, heterogeneous nucleation occurs more readily than homogeneous nucleation and is responsible for the majority of primary nucleation in crystallization processes.

Secondary nucleation is the formation of new crystals in the presence of existing crystals. This type of crystallization can be attributed to fluid shear or to collisions between already existing crystals with either a solid surface (e.g. agitator) or with each other. Attrition is the dominant form of nucleation in industrial crystallization processes.[3]

#### 2.2.2.2 Nucleation kinetics

The electric field does not only affect the nucleation work, but also the nucleation kinetics. The basic idea is that an electric field could orientate (align) solute molecules within the solution, so that one specific crystal structure can be obtained. Ziabicki et al. investigated nucleation for polar and non-polar crystals in the presence of a DC electric field. It was found that polar crystals with permanent dipole moment are highly sensitive to the electric field, whereas non-polar crystals have a negligibly small interaction with the electric field. This is due to the fact that compounds with a permanent dipole moment have an intrinsic charge distribution, so that the electric field can affect the orientation manner of a solute molecule in solution. In that sense an electric field could align polar crystals parallel to the field. It was observed that in the presence of an external electric field, formation of polar crystals parallel to the field was strongly enhanced, where formation of perpendicular or antiparallel crystals was practically eliminated. Thus, a more narrow crystal orientation distribution was obtained due to the presence of an electric field. It had no significant

effect on the formation of non-polar crystals, because it cannot affect the orientation of these solute molecules. This is due to the fact that these crystals have little interaction with the field, because there is no net charge distribution present in these molecules. The effect of the electric field on molecular orientation in solution is depicted in figure 3.[6]

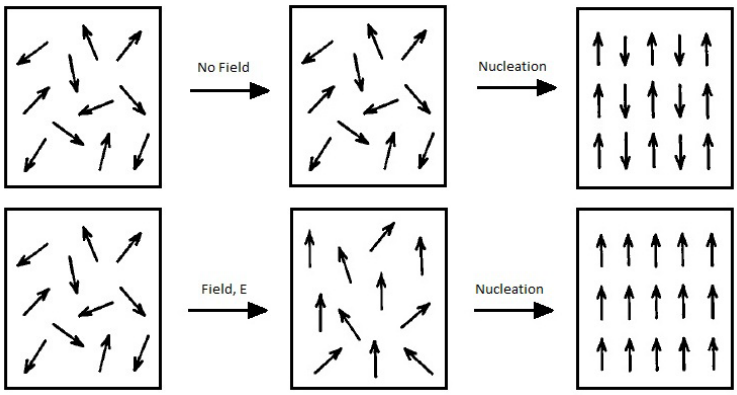


**Figure 3: The electric field effect on nucleation kinetics. In the absence of an electric field, no orientation of the solute molecules is observed. In the presence of an electric field, the solute molecules show an orientation effect which leads to parallel crystals within the structure.**

### 2.2.2.3 Local supersaturation

A local concentration gradient is the final effect of an electric field on a supersaturated solution that is discussed. Local supersaturation can be achieved, for example, by solving proteins in a particular solution at certain conditions. If the conditions are so, that the protein is charged (e.g. zwitterion form) than it is possible that under the influence of an electric field a concentration gradient is accomplished. This can be explained by the fact that the anode attracts the negatively charged proteins so that convection occurs and locally a concentration gradients exists. This local supersaturation can induce nucleation.[7][8]

# 3. Experimental

*In section 3.1 the materials used in this research are discussed followed by an explanation of the equipment used in section 3.2. Finally, the experimental procedures used for the different types of experiments are explained in section 3.3.*

## 3.1 Materials

Isonicotinamide (INA, pyridine-4-carboxamide)[17][18][19] and 4-hydroxbenzoic acid (4-HBA) with ≥99% purity from Sigma-Aldrich was used without further purification. For the crystallization experiments different solutions were prepared with 99.8% pure 1,4-dioxane purchased from Sigma-Aldrich.

## 3.2 Equipment

### 3.2.1 Crystal16

The Crystal16 parallel crystallizer is a multiple reactor station developed by Avantium Technologies. It is an user-friendly system with simple software that performs 16 parallel crystallization experiments, with online turbidity measurements. This system is commonly used to conduct solubility, MSZW, and induction time measurements. The Crystal16 multiple reactor system can hold 16 standard HPLC glass vials (Ø 11.5 mm, flat bottomed, 1.8 mL). A building block consists of four independently heated aluminium reactor blocks encased in a robust bench top setup. These blocks are electrically heated and cooled by a combination of Peltier elements and a cryostat. The temperature range is from -15 to 100 °C and the stirring rate ranges from 0 to 1250 rpm. A picture is shown in figure 4.[20]

**Figure 4: Crystal16 multiple reactor station (Left). Crystalline parallel crystallizer (Right).**

### 3.2.2 Crystalline

The Crystalline is a parallel crystallizer developed by Avantium Technologies. It is an user-friendly system with simple software that performs crystallization experiments, with online turbidity measurements, with an on-board camera for particle viewer, and with *in situ* Raman capabilities. This system is frequently used to conduct crystal growth experiments and crystallization experiments with *in situ* Raman spectroscopy. The Crystalline facilitates 8 parallel reactors and can hold up to 8 standard disposable glass vials (Ø 16.6 mm, flat bottomed, 8 mL). Each reactor can be independently loaded, programmed, and operated. The temperature range is from -25 to 145 °C and the stirring rate ranges from 0 to 1250 rpm. The Crystalline multiple reactor station is depicted in figure 4.[20]

### 3.2.3 Crystalline multiple reactor station with coupled Raman setup

A Crystalline multiple reactor station was modified for *in situ* investigation of the applied DC electric field effect on nucleation and polymorphic transition. An on-board Raman spectroscope (HoloLab Series 5000, Kaiser Optical System, Inc., USA) was applied for the *in situ* measurements and an on-board camera system was used to visualize the crystallization process. The solution was placed in an 8 mL glass vial, with two copper wires (Ø 1 mm) present in parallel. The distance between the electrodes was 6 mm. A constant electric field ($\pm 10^5$ V $m^{-1}$) was generated by a DC power supply (FUG HCN 14, Germany). This setup offers a controlled way of cooling crystallization under influence of a strong inhomogeneous DC electric field, while turbidity measurements are performed. Appendix C gives actual photos of the setup, while a schematic is shown in figure 5.

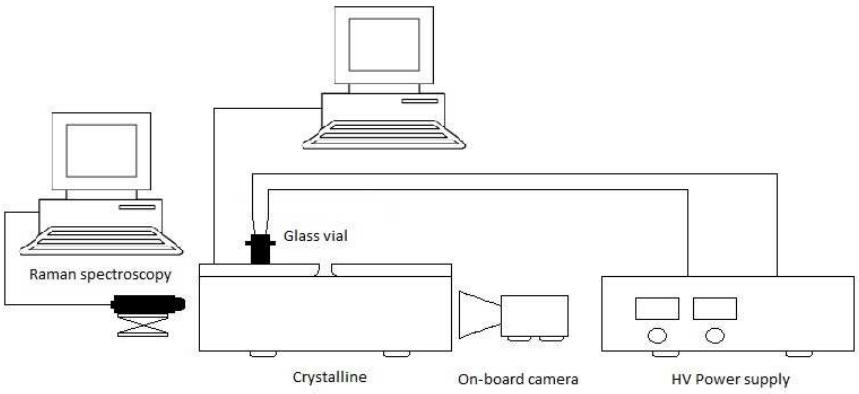


**Figure 5: Schematic picture of the Crystalline multiple reactor station with coupled Raman setup.**

### 3.2.4 Parallel-plate setup

This system was used to study the polymorphic outcome in the presence of a strong homogeneous DC electric field. It consisted of a parallel-plate setup and DC power supply (FUG HCN 14, Germany). The parallel-plate capacitor was custom built from a glass cuvette (Labomed, 45 x 12.5 x 3.5 mm, 1.7 mL) where copper electrodes (1 mm thickness) were mounted onto the inside walls of the cuvette. The distance between the electrodes was 8 mm. Within this system a more or less homogeneous electric field ($\pm 10^5$ V $m^{-1}$) was generated. Figure 6 gives a schematic overview of the experimental setup and actual photos of the setup are depicted in Appendix D. The electrodes were placed inside the solution so the dielectric constant of glass ($\varepsilon$ = 5 – 10) does not decrease the electric field strength.[21]

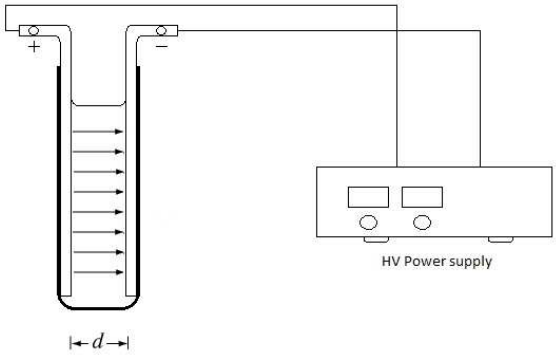


**Figure 6: Schematic picture of the parallel-plate setup.**

### 3.2.5 Characterization of crystals

**Optical analysis.** Optical images were made with a Nikon optiphot 200 optical microscope and it was used to get a first impression of the acquired crystals from the crystallization experiments. It was done in order to see if a clear distinction between polymorphic shapes was present. A scanning electronmicrograph was made with a JEOL JSM 5400 scanning electron microscope and was used to get a view on the crystal shape.

**Raman spectrometry.** Raman spectra of INA and 4-HBA crystals were recorded with a Hololab series 5000 Raman spectroscope (Kaiser Optical System, Inc., USA). The solid and *in situ* Raman spectra were recorded by excitation radiation at 785 nm using a NIR probe. *In situ* Raman spectra were recorded to find out if a polymorphic transition took place. Solid Raman spectra were recorded to determine the polymorphic form of the produced crystals. Spectra of INA crystals were acquired in the 970 to 1010 $cm^{-1}$ spectral range for extensive polymorph characterization. The characteristic pyridine ring bond vibration frequencies were used for the INA polymorph determination. Raman spectra of 4-HBA crystals were acquired in the 800 – 880 $cm^{-1}$ and the 1570 – 1630 $cm^{-1}$ spectral range, where the characteristic –OH bend frequency and the C=O stretch frequency were used for the 4-HBA polymorph determination.

**X-ray powder diffraction.** X-ray powder diffraction patterns were taken using a Bruker D5005 diffractometer with Cu Kα radiation (λ = 0.154 nm) with 0.038° resolution in 2θ. Measured patterns are matched to the CSD database. X-ray powder diffraction was executed in order to determine the crystal structure of the produced materials.

**DSC and TGA.** Differential scanning calorimetry (DSC) and thermogravimetric analysis (TGA) were used to characterize the thermal behavior of the produced crystals. A Perkin Elmer DSC7 was used to measure phase transitions (endo- or exothermic energy upon heating) within the system. The samples were measured in a nitrogen atmosphere, with a heating rate of 5 °C $min^{-1}$ and a purge rate of 20 mL $min^{-1}$. A Perkin Elmer TGA7 was used to measure the thermal stability upon heating. The samples were measured in a nitrogen atmosphere, with a heating rate of 10 °C $min^{-1}$ and a purge rate of 20 mL $min^{-1}$.

## 3.3 Experimental procedures

### 3.3.1 Solubility measurements

Crystal16 was used to determine the INA and 4-HBA solubility in 1,4-dioxane. The turbidity sensor detected the clear and cloud points in each reactor, which indicated the saturation and recrystallization temperature, respectively. Suspensions of the compounds with different concentrations were prepared by adding a known amount of crystalline material and 1 mL solvent in the 16 HPLC vials containing a magnetic stirring bar. The heating rate was set to 1 °C $min^{-1}$ and the cooling rate was set to 0.5 °C $min^{-1}$, while the stirring speed was maintained at 700 rpm. The temperature at which the suspension becomes a clear liquid was taken as the saturation temperature and it was measured 3 times per sample, by cycles of cooling and reheating. The cloud point refers to the point at which solid material first appears upon a decrease of temperature.[22]

### 3.3.2 Induction time measurements

Induction time measurements were performed in the absence and presence of an electric field. It was only done for the model compound INA. Crystal16 was used for induction time measurements in the absence of an electric field, while the Crystalline was used to measure the induction time in the presence of the electric field.

In the absence of an electric field the induction time was measured at three different concentrations (25, 30, and 35 mg $mL^{-1}$). For all measurements at one supersaturation ratio a 30 mL solution was prepared by dissolving the corresponding amount of the model compound in the solvent (1,4-dioxane). Then in all 16 HPLC vials 1 mL of solution was dispensed. The suspensions were heated to a clear solution with a heating rate of 0.5 °C $min^{-1}$. This clear solution was rapidly cooled down to 25 °C with a cooling rate of 5 °C $min^{-1}$. The induction time was taken as the moment at which the solution transmission decreased. The holding temperature at 25 °C was at most 4 hours. To make sure that all crystals were dissolved the sample was stirred for at least 30 minutes at the highest temperature. During the experiment the stirring speed was maintained at 700 rpm. Then, the sample was reheated with a rate of 0.5 °C $min^{-1}$ to dissolve the crystals and start another cycle. To obtain representative results, the cold-heat cycle was repeated 4 times. This means that 64 induction time measurements were performed under identical conditions for each supersaturation ratio.[22]

Induction time experiments in the presence of the electric field were performed at a concentration of 35 mg $mL^{-1}$. This is done in order to verify if the electric field affects the induction time. A 100 mL solution was prepared by dissolving the corresponding amount of INA in 1,4-dioxane. Then 4 mL of solution was dispensed in a 8 mL standard disposable vial. The suspension was heated to a clear solution with a heating rate of 1 °C $min^{-1}$ and, upon heating, the electric field ($\pm 10^5$ V $m^{-1}$) was generated. The clear solution was cooled down to 25 °C with a cooling rate of 5 °C $min^{-1}$. During the experiment a constant potential difference of +7.5 kV was maintained. To obtain representative results, this experiment was repeated 20 times.

### 3.3.3 Crystalline multiple reactor station with coupled Raman setup

Different concentrations of INA (17, 20, 30, and 35 mg $mL^{-1}$) solved in 1,4-dioxane were examined at different cooling rates in the absence or in the presence of an electric field. All the experimental solutions were in the metastable zone in order to prevent uncontrolled nucleation. At each concentration experiments were conducted for different cooling rates (0.3, 0.5, 1, 3, and 5 °C $min^{-1}$) in the absence or the presence of an electric field. In the absence of the electric field 3 mL samples were heated up to 60 °C with a constant heating rate of 2 °C $min^{-1}$ to acquire a clear solution. Then the clear solution was cooled down to 12 °C at a certain cooling rate. The holding temperature at 12 °C was at most 4 hours. During the experiment a constant stirring rate of 700 rpm was maintained and a Raman spectroscope recorded the *in situ* spectra. The same experiments were conducted in the presence of an electric field, except no stirring was present. During these experiments a constant potential difference of +7.5 kV was maintained, which created a field strength in the order of $10^5$ V $m^{-1}$.

This experiment was repeated with 4-HBA at a concentration of 160 mg $mL^{-1}$ with a cooling rate of 1 °C $min^{-1}$ in the absence and presence of an electric field. A 3 mL suspension was heated up to 65 °C with a heating rate of 2 °C $min^{-1}$ to get a clear solution, subsequently the solution was cooled down to 20 °C with a cooling rate of 1 °C $min^{-1}$. The holding temperature at 20 °C was at most 4 hours. In

the absence of an electric field a stirring rate of 700 rpm was maintained, while in the presence of an electric field no stirring was applied. A prevailing potential difference of +7.5 kV was maintained, which created a field strength in the order of $10^5$ V $m^{-1}$.

### 3.3.4 Parallel-plate setup experiments

Isonicotinamide was the only model compound tested in this system. Solutions with different concentrations (30 and 35 mg $mL^{-1}$) were tested in the parallel-plate capacitor. Beforehand, a 20 mL solution was prepared by dissolving the corresponding amount of INA in 1,4-dioxane. Then, 1 mL of solution was dispensed in the parallel-plate setup and heated until a clear solution was obtained. Subsequently, the clear solution was (in the absence of an electric field) cooled in air, water, and ice water, respectively. These experiments were repeated, but with agitation present in the system. For agitation a magnetic stirring bar was used. The effect of supersaturation, cooling rate, and agitation on the crystallization process was investigated in the absence of an electric field in this system.

The same procedure was taken for experiments in the presence of an electric field (no agitation, cooled with air), where three different potential differences (5, 7.5, and 10 kV) were applied to the system. These potential differences created a field strength in the order of $10^5$ V $m^{-1}$. Appendix E gives the actual field strengths present at these conditions. The effect of electric field strength on the crystallization process and polymorphic outcome was investigated in this system. All crystals obtained during these experiments were investigated under the optical microscope and scanning electron microscope.

# 4. Results and Discussion

*This section describes the results obtained from the various experiments which were performed. Section 4.1 gives the outcome of the literature survey done on material selection. The solubility and MSZW were determined for the model compounds in the proper solvent, which is explained in section 4.2. The next section 4.3 describes the effect of the electric field observed by the Crystalline setup and section 4.4 describes the electric field effect observed in the parallel-plate setup. Finally, in section 4.5 the electric field effect on induction time is discussed.*

## 4.1 Material selection

An essential step in understanding the crystallization behavior and conducting experiments is the characterization of materials. Material selection was important, because crystallization in the presence of an electric field imposes different requirements on the system and its compounds. Knowledge of the thermodynamic and kinetic properties is therefore of vital importance. In this section the properties of the two model compounds and the solvent selection procedure are addressed. The compounds isonicotinamide (INA) and 4-hydroxybenzoic acid (4-HBA) were used for experiments.

Isonicotinamide possesses strong anti-tubercular, anti-pyretic, and anti-bacterial properties.[19] It is commonly used as a co-former in co-crystallization for tuning the physical properties (e.g. bioavailability) of drug molecules. This is being investigated for Huntington's disease and anti-inflammatory activity.[23] Isonicotinamide is used in this research, because it possesses favorable properties such as a distinct polymorphic shape and a high dipole moment (3.56 D). It is convenient to have a distinct polymorphic shape, because it simplifies the analysis of the crystals. A high dipole moment is necessary because the electric field could have a strong influence on the orientation of a molecule. Currently, there are six known polymorphs of INA. The stable polymorph (Form II) forms INA dimers and all metastable polymorphs are arranged as chains, which is depicted in figure 7.

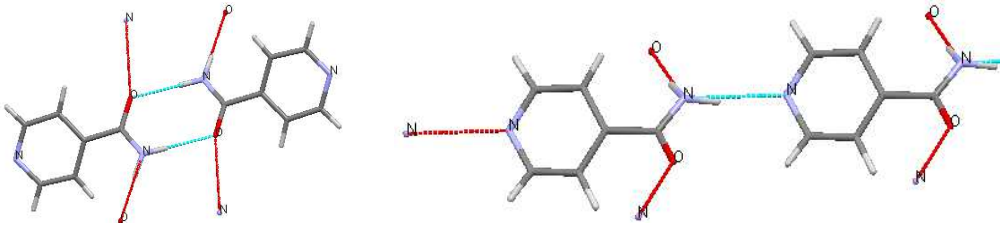

**Figure 7: Stable form II (dimer structure) of INA with hydrogen bond motifs (left) and a metastable form (chain-like structure) of INA with hydrogen bond motifs (right).**

4-Hydroxybenzoic acid is primarily known as the basis for the preparation of its ester, which is used as a preservative in cosmetics and ophthalmic solutions. It is used in this research, because it has distinct polymorphs and a high dipole moment (3.35 D). Currently, there are two known polymorphs of 4-HBA and also for this compound the stable polymorph has a dimer like structure, whereas the metastable form has a chain like structure.

In designing an optimized crystallization process under influence of an electric field it is essential to select the proper solvent. In this research solvent selection is based on interaction with the electric field. In order to reduce the solvent interaction with the electric field it was important to choose a solvent, which had a low dielectric constant and dipole moment. A low dielectric constant is favorable, because the solvent acts like a capacitor within the system and thereby lowering the elctric field strength. So higher electric field strengths can be obtained in the crystallization system if the solvent features a low dielectric constant. From literature it is known that an electric field strength in the order of $10^5 – 10^7$ V $m^{-1}$ is necessary to induce nucleation or align molecules.[10][24][25]

A low dipole moment is desired, because then the electric field effect on the solvent structure is minimal. So possible solvents are preferably non-polar with a low dielectric constant. For practical reasons other properties such as viscosity, boiling temperature, melting temperature, and toxicity are also considered. Non-polar 1,4-dioxane was chosen as a solvent due to its favourable dielectric properties. Appendix F thoroughly discusses the solvent selection. In conclusion, great care was taken to choose materials that are suitable for crystallization under the influence of a DC electric field.

## 4.2 Compound characterization

With the proper materials known, it was important to measure their solubility. Solubility is the saturation concentration of a substance in a solvent obtained by determining the maximum amount that is soluble. The solubility curve gives the temperature dependence of the solubility of a compound in a solvent. It is an excellent starting point, because it gives an indication of the concentrations (or supersaturation ratio) to use for crystallization experiments. Metastable zone width (MSZW) is an important parameter in nucleation behaviour and it is defined as the difference between the saturation temperature and the temperature at which crystals are detected upon cooling the solution with a certain cooling rate.[12] The solubility line and MSZW were determined for both model compounds in 1,4-dioxane.

Figure 8 shows the solubility (blue line) and MSZW (red line) of INA in 1,4-dioxane. Cloud points were measured in threefold and are depicted as scatter in the figure. An averaged value was taken to construct the MSZW. The concentration is highly temperature dependent, so cooling crystallization is the best crystallization technique for this system. Indications for a polymorphic system with two enantiotropic polymorphs can be observed, because a possible transition temperature is visible at 44.2 °C. Although to be certain one has to conduct more experiments such as solubility (e.g. in the region of the transition point) and XRPD measurements. Most experiments during this study were performed in the MSZW, where no spontaneous nucleation can occur in order to examine the electric field effect on crystal nucleation behaviour and polymorphic outcome.

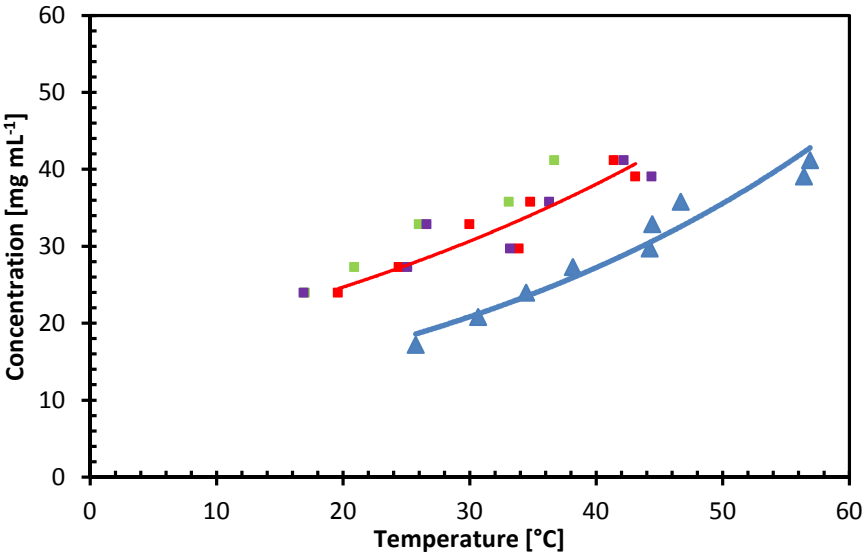


Figure 8: Solubility curve of INA (blue line) with the metastable line (red line) in 1,4-dioxane as a function of temperature. The space between these curves is defined as the MSZW.

The solubility (blue line) and MSZW (red line) of 4-HBA in 1,4-dioxane is depicted in figure 9. Also for this system concentration is very temperature dependent, which suggests that cooling crystallization is the best crystallization technique for this system. A possible transition temperature can be observed at 39.2 °C, which indicates that a polymorphic system with two enantiotropic polymorphs may be present. Although to be certain one has to conduct more experiments such as solubility (e.g. in the region of the transition point) and XRPD measurements.

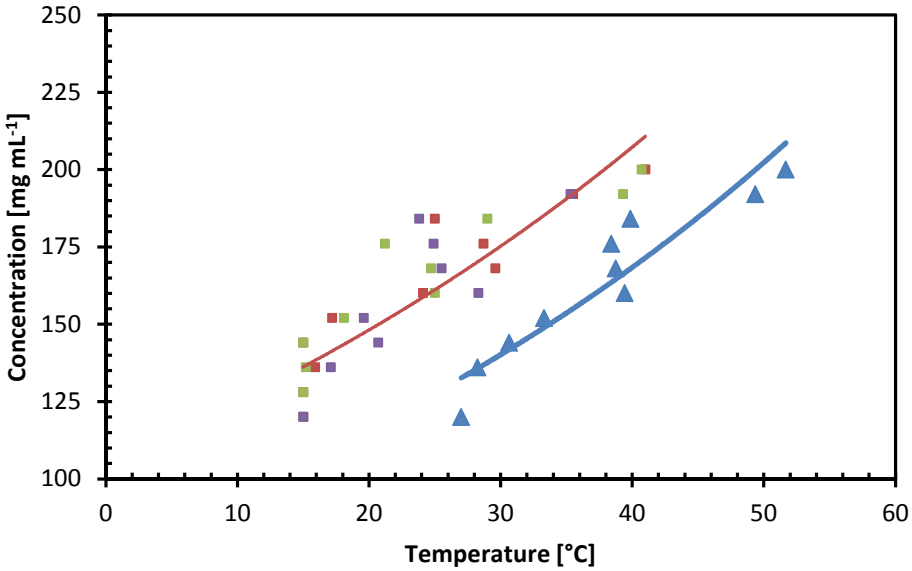


Figure 9: Solubility curve of 4-HBA (blue line) with the metastable line (red line) in 1,4-dioxane as a function of temperature. The space between these curves is defined as the MSZW.

## 4.3 Effect of the electric field observed by the Crystalline setup

To understand and discuss the electric field effect on the crystallization process a new experimental setup was built for *in situ* investigation of the effect of a strong electric field on nucleation and polymorphic transition. Experiments with the Crystalline multiple reactor system (with an on-board camera and a coupled Raman spectroscope) investigated the influence of crystallization parameters such as the supersaturation ratio, cooling rate, agitation and electric field strength on the crystallization process. Two polymorphic systems (INA and 4-HBA in 1,4-dioxane) were examined in this new experimental setup. Firstly, the observed effects in the absence of an electric field are reviewed and subsequently the observations in the presence of an electric field are discussed. During the experiments *in situ* Raman spectra were recorded and the crystals were analyzed with solid Raman spectroscopy, X-ray powder diffraction, and differential scanning calorimetry.

### 4.3.1 Experiments in the absence of the electric field

Measurements conducted for several INA concentrations (17, 20, 30, and 35 mg $mL^{-1}$) at well-controlled cooling rates (0.3, 0.5, 1, 3, and 5 °C $min^{-1}$) and at a constant stirring rate of 700 rpm and in the absence of the electric field resulted in understanding the influence of the crystallization parameters on the system. This experiment was also repeated with 4-HBA at a concentration of 160 mg $mL^{-1}$ with a cooling rate of 1 °C $min^{-1}$ in the absence of an electric field.

It was observed that with increasing concentrations and cooling rates, MSZW decreased due to a higher prevailing driving force. Interestingly, it was also noticed that with declining cooling rates bigger crystals were acquired with a more nicely faceted crystalline shape. This effect can be attributed to the fact that solute molecules in solution have more time to incorporate into the crystal structure under small driving force conditions. Heterogeneous nucleation and crystal growth took place throughout the system, which means that crystals formed on the glass wall of the vial, electrodes, and the gas-liquid interface. Homogeneous nucleation was not observed.

### 4.3.2 Experiments in the presence of the electric field

Experiments in the presence of an electric field were conducted for two different INA concentrations (17 and 35 mg $mL^{-1}$) at different cooling rates (0.3, 0.5, 1, 3, and 5 °C $min^{-1}$) and at a constant potential difference of +7.5 kV. It was observed that crystallization did not occur at any cooling rate for the lowest concentration. One must bear in mind that the holding time at this concentration was several hours (± 6 hours) and not days. It may be possible that crystallization would have taken place after this holding time, but that is not investigated. However, this is in sharp contrast with the previous experiment, which was in absence of the electric field, where crystallization did occur at this concentration. It can be stated that the electric field affects the crystallization process. One possible explanation for this observation is that the electric field has an effect on the nucleation work in such a way that the Gibbs free energy is increased so that the driving force cannot overcome this energy barrier (eq. **2-4**). Another explanation for this is that the electric field enhances the induction time. This could happen if the dielectric constant of the solution exceeds the dielectric constant of the crystalline phase ($\varepsilon_S > \varepsilon_c$). One cannot state this for certain, because according to theory the dielectric constant of both phases are nearly equal and so the induction time should remain constant.

For experiments performed at C = 35 mg $mL^{-1}$ crystallization occurred for cooling rates equal to or greater than 1 °C $min^{-1}$. This proves that the degree of supersaturation is very important for the nucleation process to occur. With the on-board camera system crystal growth was only observed at

the electrodes (mainly on the anode; see figure 10). There were no visible crystals at other locations and these results correspond with other findings in literature, where crystals also grew on one particular electrode.[8] This can be elucidated by the fact that the electric field can induce a dipole moment. The anode attracts the negatively charged compound so that convection occurs and locally a concentration gradient exists. In this way crystallization could take place only on the anode.

An experiment was executed with 4-HBA at C = 160 mg $mL^{-1}$ with a cooling rate of 1 °C $min^{-1}$ and at a constant potential difference of +7.5 kV. In the presence of the $10^5$ V $m^{-1}$ electric field crystals appeared mainly on the anode.

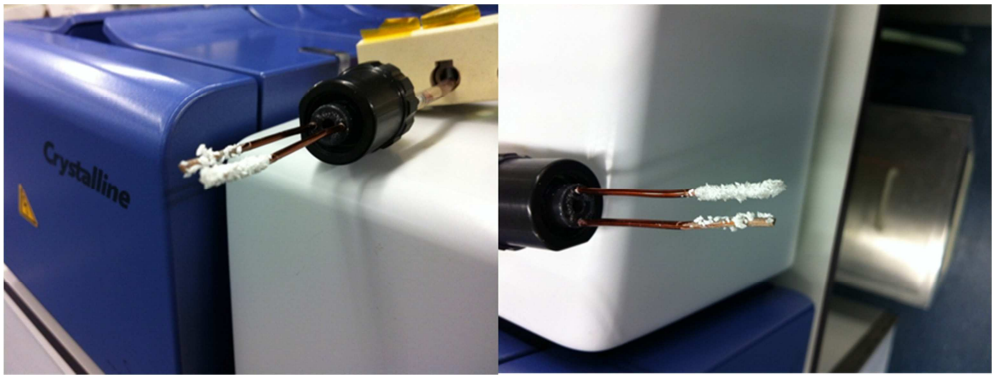


**Figure 10: Two pictures of the crystal formation on the electrodes. It is visible that on one electrode (anode) more crystals are formed.**

Crystals from the anode and cathode were obtained separately to see whether the electrode type has influence on crystal structure formation. Solid Raman spectra of INA and 4-HBA crystals acquired from the anode and cathode showed no difference, which is depicted in appendix G. One can conclude that the electrode type does not influence the polymorphic structure.

### 4.3.3 Discussion

Solid Raman spectra of INA and 4-HBA crystals (obtained from the anode) were recorded to determine the polymorphic form. The measured spectra of the crystals acquired in the absence and in the presence of the electric field were compared to the purchased material. The INA crystals were obtained from recrystallization in 1,4-dioxane with a prevailing concentration of C = 35 mg $mL^{-1}$, cooling rate 1 °C $min^{-1}$, and (if present) ΔV = +7.5 kV. The conditions for the produced 4-HBA crystals were C = 160 mg $mL^{-1}$, cooling rate 1 °C $min^{-1}$, and (if present) ΔV = +7.5 kV.

Figure 11 shows the solid Raman spectra of the INA crystals obtained from a cooling crystallization experiment (with and without the electric field present; ± $10^5$ V $m^{-1}$) and purchased INA. Raman spectra of different INA polymorphs show differences in the pyridine region between 970 and 1010 $cm^{-1}$. The Raman peak indicates the ring breathing mode of the pyridine, which includes ring vibration and ring bond stretching. The stable polymorph gives a peak at 991 $cm^{-1}$, where metastable forms show a peak maximum between 995 – 998 $cm^{-1}$.[26] The purchased INA (blue line) shows a peak at 991 $cm^{-1}$, so it is the stable form II. From recrystallization experiments in 1,4-dioxane in the absence of an electric field (orange line) a peak is present at 997 $cm^{-1}$, which indicates that a metastable form is obtained. For recrystallization experiments under influence of the electric field (green line) peaks at 991 $cm^{-1}$ and 997 $cm^{-1}$ are displayed, which indicates a mixture of both polymorphs.

It is observed that the polymorphic outcome is changed from purely a metastable form (in the absence of the electric field) to a mixture of the stable and metastable form (in the presence of the electric field). This observation suggests that a strong DC electric field affects the polymorphic outcome of a cooling crystallization experiment. Due to the presence of an electric field, solute molecules in solution are more aligned than in the absence of an electric field. This means that the electric field has an effect on the orientation of the solute molecules. The alignment of solute molecules causes that one specific polymorphic form is preferred or energetically favorable over the other polymorphic forms. For example, the INA molecules in solution crystallized to a metastable form in the absence of an electric field, but under the influence of the electric field INA molecules were oriented in such a way that a mixture of both the stable and a metastable polymorph was produced. Also one could imagine that when the solute molecules are more aligned, the number of effective collisions (frequency factor) and thereby the nucleation rate (eq. **2-6**) could increase. In this case the electric field strength was not strong enough to produce only the stable polymorph, but with an enhanced field strength it would be possible. This result may in the future, for instance, be used in the pharmaceutical industry in order to control the polymorphic outcome of a cooling crystallization process.

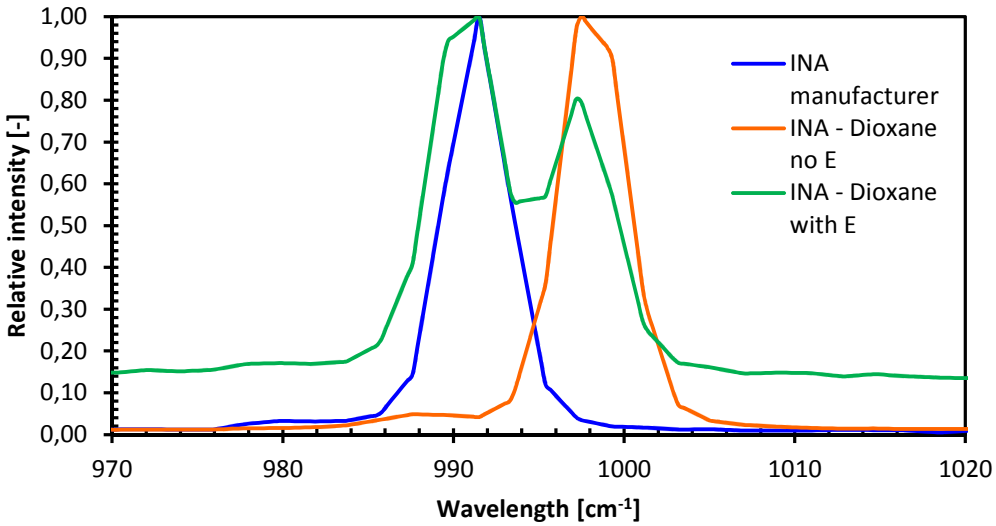


**Figure 11: Solid Raman spectra given for INA crystals obtained from the manufacturer (blue line), recrystallized in the absence of an electric field (orange line), and recrystallized in the presence of an electric field (green line).**

X-ray powder diffraction confirmed that the purchased INA was indeed the stable form II and that the crystals acquired in the absence of the electric field were the metastable form I (appendix H displays the XRPD patterns). DSC analysis confirmed that two different polymorphs are obtained, which is shown in figure 12. The DSC trace for recrystallized INA crystals exhibited a single endothermic peak at 159.2 °C, representing fusion (melting). For the purchased INA, the DSC trace exhibited an initial endothermic peak at 120.6 °C, followed by a second endothermic peak at 156,8 °C. The first peak indicates a solid-solid phase transition from the stable polymorph to a metastable form and the second peak represents melting. This means that the polymorphs are enantiotropically related.

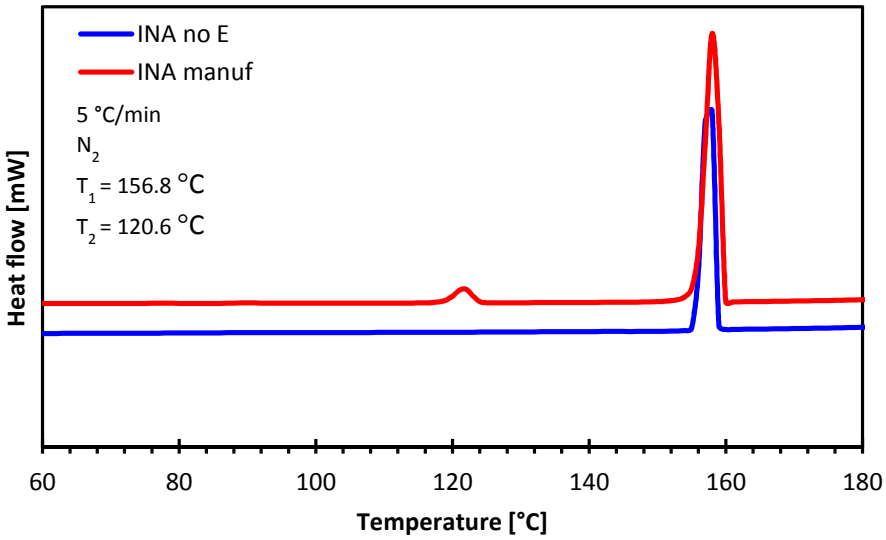


Figure 12: DSC traces of INA recrystallized in the absence of an electric field (blue line) and the purchased INA (red line).

TGA validated that no pseudo-polymorphs such as solvates are obtained. The TGA data is given in appendix I.

Figure 13 depicts the *in situ* solution Raman spectra recorded during the INA cooling crystallization experiments. The left spectrum was recorded under the conditions of C = 35 mg $mL^{-1}$, cooling rate of 1 °C $min^{-1}$, and in the absence of an electric field. The right spectrum was obtained under the same conditions with the exception that an electric field was present. Both graphs show peaks at 991 and 1010 $cm^{-1}$, in which the first peak indicates the INA molecules and the second peak is a characteristic peak for 1,4-dioxane. Both *in situ* Raman spectra showed no polymorphic transition. It was expected that in the absence of the electric field a transition was shown from the stable to the metastable form, because solid Raman spectra proved that a metastable polymorph of INA was obtained. In the presence of the electric field a transition was expected to occur due to the electric field effect on the orientation of solute molecules. Whenever the electric field strength was strong enough to affect the alignment of the molecules (and an effect on the polymorphic outcome was measured), a polymorphic transition was expected to occur, because this alignment would cause one specific polymorph to be obtained.

There are two main reasons why a transition is not observed. The first reason is that crystal formation took place on the electrodes and not within the solution. The Raman laser was directed to the middle of the solution (between the electrodes) and so the produced crystals on the electrodes were not detected by the Raman laser. According to Kulkarni et al. the INA molecules could arrange themselves in 1,4-dioxane as chain-like structures (metastable polymorphs) or as single molecules. Apparently, INA molecules do not form chain-like structures (otherwise a peak at 998 $cm^{-1}$ was observed), but single molecules are present in 1,4-dioxane.[26] The single molecules travel to the electrode where cluster formation takes place and eventually lead to crystal formation on the electrodes and this is the second reason why no polymorphic transition was seen.

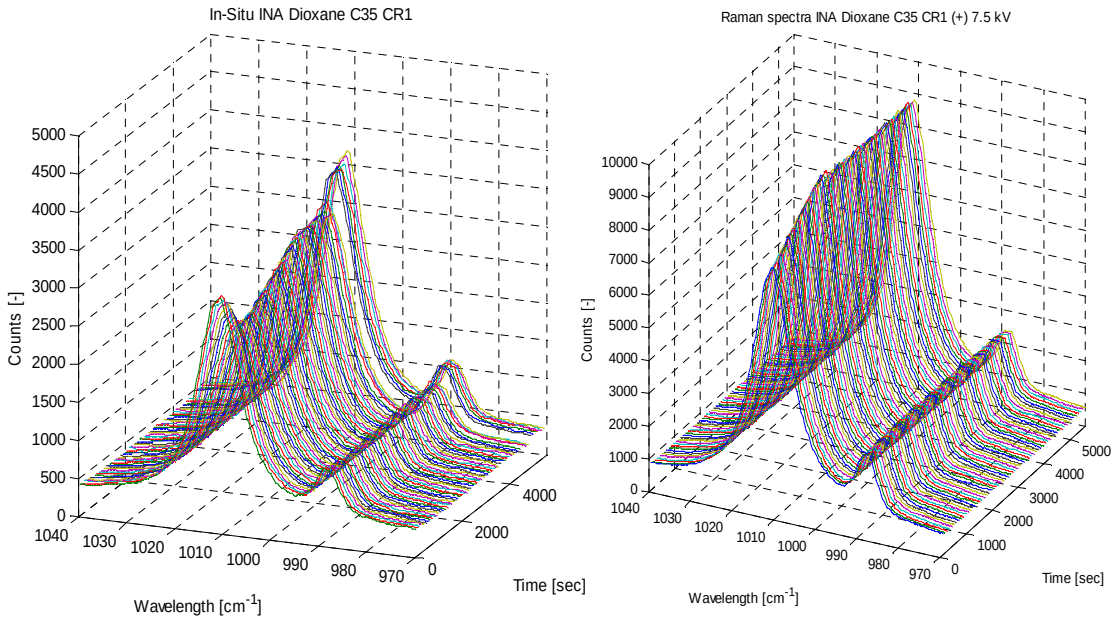


**Figure 13: Recorded *in situ* solution Raman spectra of INA in the absence of the electric field (left) and in the presence of the electric field (right). Characteristic peak for INA at 990 $cm^{-1}$.**

Figures 14 and 15 show the solid Raman spectra of the 4-HBA crystals obtained from a cooling crystallization experiment (with and without the electric field present; ± $10^5$ V $m^{-1}$) and purchased 4-HBA. Raman spectra of different 4-HBA polymorphs show differences in the –OH region between 800 – 880 $cm^{-1}$ and in the C=O group region between 1570 – 1630 $cm^{-1}$. The Raman peaks indicate the bending of the –OH group and the stretching of the C=O group, respectively. The stable polymorph gives Raman peaks at 836 , 849, 1594, 1606 $cm^{-1}$ where the metastable form shows maximum peaks at 826, 845, 1584, 1601 $cm^{-1}$. The measured Raman shift in the –OH region is displayed in figure 14. The purchased 4-HBA (blue line) shows peaks at 836 and 849 $cm^{-1}$, so it is the stable form. Recrystallizing in 1,4-dioxane (red line) acquires peaks at 826, 836, 845, and 849 $cm^{-1}$, which indicates a mixture of both polymorphs. From recrystallization under the influence of the electric field (green line) peaks at 826 and 845 $cm^{-1}$ are shown, which means a metastable polymorph is formed. The same trend is seen in the C=O region and is depicted in figure 15.

It is observed that the polymorphic outcome is changed from a mixture of both polymorphs (in the absence of the electric field) to purely a metastable form (in the presence of the electric field). This observation suggests that a strong DC electric field affects the polymorphic outcome of a cooling crystallization experiment. It could be explained by the fact that the electric field influences the orientation of solute molecules in solution in such a way that they are more aligned. This alignment causes that one particular polymorphic form is favorable over the other form, so that one specific polymorph is produced (in this case the electric field strength was sufficient to align the molecules so that only the metastable form was obtained).

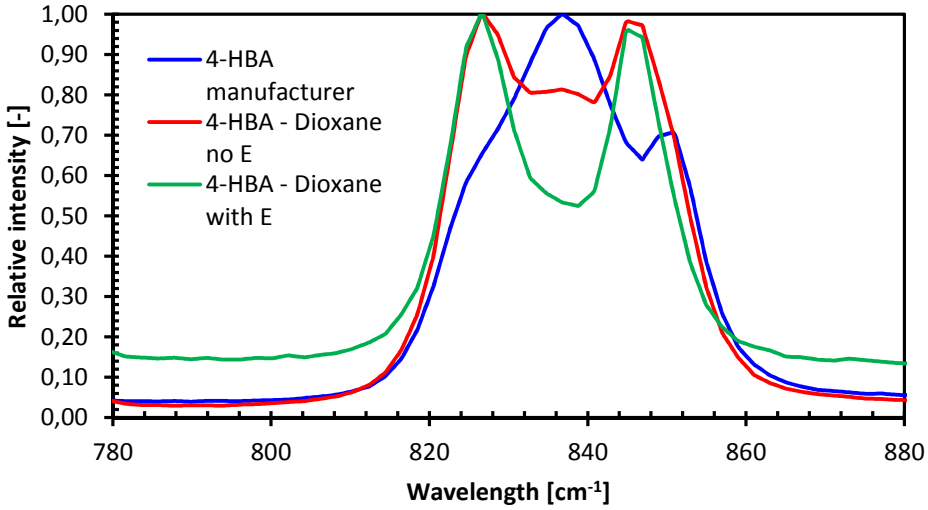


**Figure 14: Solid Raman spectra given for 4-HBA crystals obtained from the manufacturer (blue line), recrystallized in the absence of an electric field (red line), and recrystallized in the presence of an electric field (green line). This spectral range indicates the differences in the –OH region.**

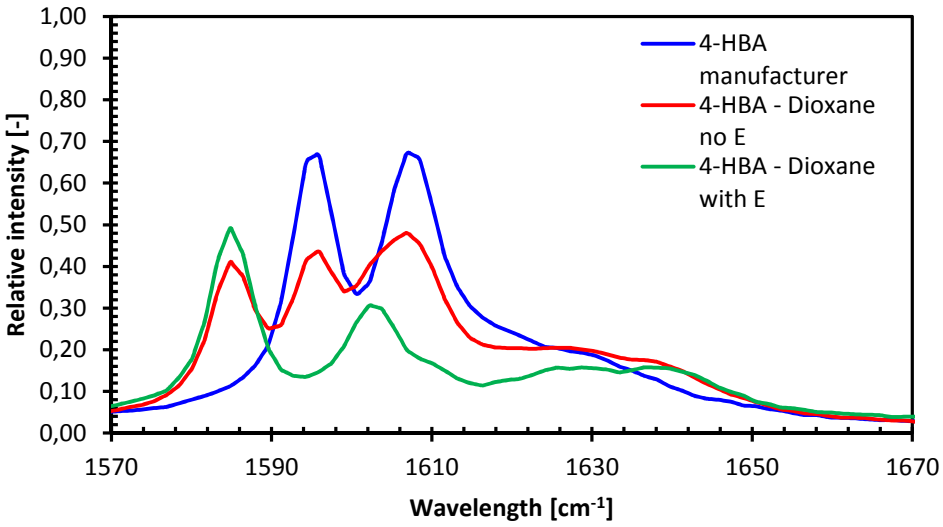


**Figure 15: Solid Raman spectra given for 4-HBA crystals obtained from the manufacturer (blue line), recrystallized in the absence of an electric field (red line), and recrystallized in the presence of an electric field (green line). This spectral range indicates the differences in the C=O region.**

X-ray powder diffraction confirmed that the purchased 4-HBA was indeed the stable polymorph, that the crystals acquired in the absence of the electric field were a mixture of both polymorphs, and that the crystals acquired in the presence of the electric field were the metastable form. DSC analysis showed no difference between all three samples, which is depicted in figure 16. The DSC trace for the purchased 4-HBA exhibited an initial endothermic peak at 214.7 °C, followed by a second endothermic peak at 236.4 °C. The same holds for the DSC traces of recrystallized 4-HBA crystals in the absence and in the presence of an electric field.

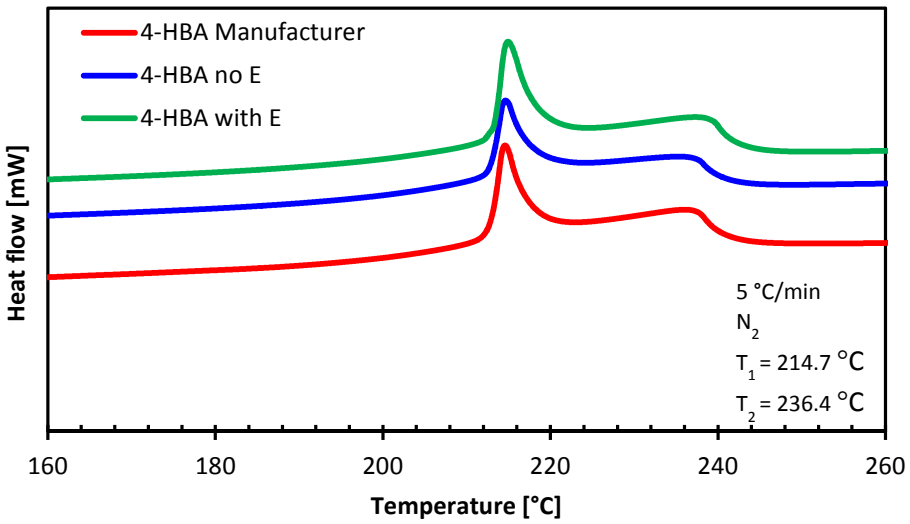


**Figure 16: DSC traces of 4-HBA recrystallized in the presence of an electric field (green line), recrystallized in the absence of an electric field (blue line), and the purchased 4-HBA (red line).**

The *in situ* solution Raman spectra recorded during the 4-HBA cooling crystallization experiments are depicted in figures 17 and 18. Figure 17 showed the characteristic peaks for the stable polymorph at 836 and 849 $cm^{-1}$ and figure 18 for peaks at 1594 and 1606 $cm^{-1}$. The left spectra were recorded under the conditions of C = 35 mg $mL^{-1}$, cooling rate of 1 °C $min^{-1}$, and in the absence of an electric field. The right spectra were obtained under the same conditions, but with the exception that an electric field was present. Both *in situ* Raman spectra showed no polymorphic transition. It was expected that in the absence of the electric field a transition was shown from the stable form to a mixture of both forms, because solid Raman spectra proved that a mixture of both polymorphs of 4-HBA was obtained. In the presence of the electric field a transition was expected to occur due to the electric field effect on the orientation of solute molecules. This alignment would cause one specific polymorph to be obtained, so a transition of one polymorph to another was expected.

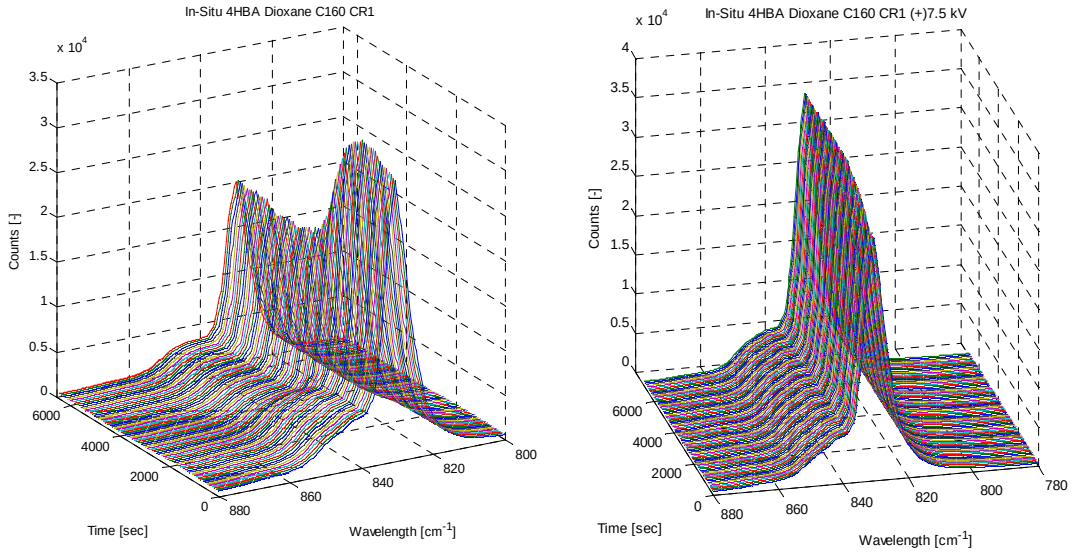


**Figure 17: Recorded *in situ* solution Raman spectra of 4-HBA in the absence of the electric field (left) and in the presence of the electric field (right). Characteristic peaks at 836 and 849 $cm^{-1}$.**

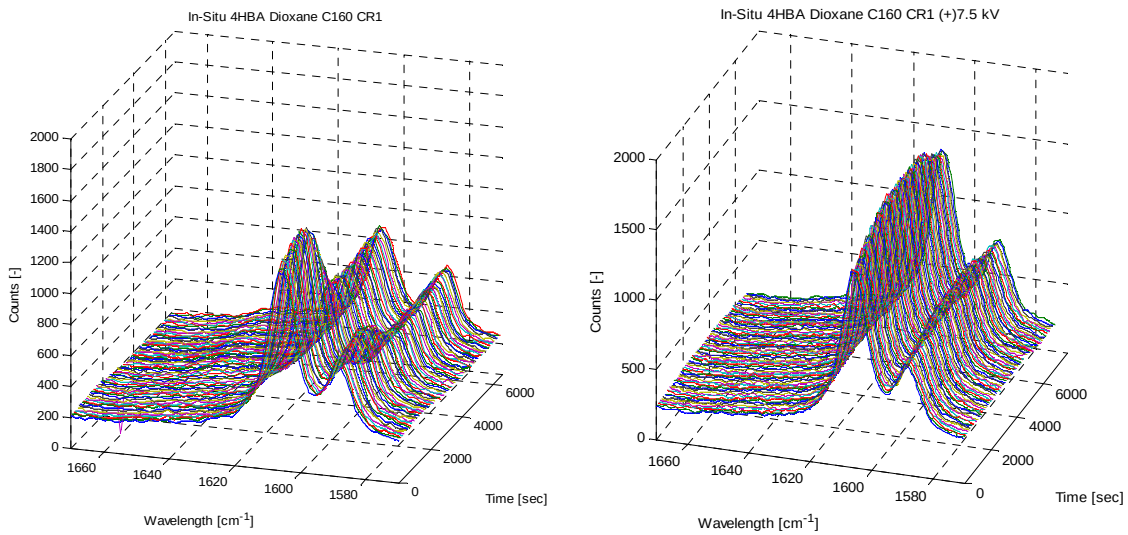


**Figure 18: Recorded *in situ* solution Raman spectra of 4-HBA in the absence of the electric field (left) and in the presence of the electric field (right). Characteristic peaks at 1594 and 1606 $cm^{-1}$.**

The main reason why a polymorphic transition is not observed is due to the fact that crystal formation took place on the electrodes and not within the solution. The Raman laser was directed to the middle of the solution (between the electrodes) and so the produced crystals on the electrodes were not detected by the Raman laser. In this way Raman spectroscopy does not record a polymorphic transition.

## 4.4 Effect of the electric field observed by the parallel-plate setup

The parallel-plate setup had the advantage of generating a more homogeneous electric field than could be created in the Crystalline multiple reactor system. Experiments (in the absence of the electric field) were performed to investigate the influence of primary nucleation factors such as supersaturation ratio, agitation, and cooling rate. Finally, the electric field effect is examined at pre-determined conditions. Aim was to check if the electric field strength had an influence on the polymorphic outcome. It must be noted that in this experimental setup only INA was used as a model compound to carry out experiments.

### 4.4.1 Experiments in the absence of the electric field

The influence of primary nucleation factors were investigated in the absence of the electric field. Solutions of different concentrations (30 and 35 mg $mL^{-1}$) were cooled down with air, water, and ice water, respectively. These experiments were repeated with agitation present. The results obtained without the presence of an electric field are summarized in table 1.

**Table 1: Summarized results of the experiments performed in the absence of an electric field.**

| **C = 35 mg $mL^{-1}$** | **Cooling rate** | | | **Agitation (air cooled)** | |
|---|---|---|---|---|---|
| | **Air** | **Water** | **Ice water** | **Yes** | **No** |
| Nucleation time | ± 20 min | ± 10 min | ± 1 min | ± 20 min | ± 20 min |
| Polymorphic outcome | Form III | Form III | Form III | Form III | Form III |
| Mean particle size [µm] | 550 | 550 | 550 | 50 | 550 |

Experiments conducted at both concentrations showed no difference due to the fact that both concentrations either lie on the metastable line or in the spontaneous nucleation region. Cooling rate affected the time it took for crystals to appear in solution. With higher cooling rates, faster nucleation occurred which is due to a higher prevailing driving force. The presence of a magnetic stirring bar resulted in crystals with a much lower mean particle size. It must be noted that the polymorphic outcome was analyzed by single-crystal diffraction. This analysis showed that polymorphic form III was present, but also a small amount of opaque material which could not be analyzed by single-crystal analysis.

### 4.4.2 Experiments in the presence of the electric field

A stagnant solution (C = 35 mg $mL^{-1}$) was air cooled in the presence of an electric field. Experiments were conducted at three different potential differences (5, 7.5, and 10 kV), which created a homogeneous electric field in the order of $10^5$ V $m^{-1}$. Actual electric field strengths are presented in appendix E. X-ray powder diffraction was carried out in order to determine the polymorphic form of the acquired crystals.

The obtained XRPD patterns of the 5 and 7.5 kV experiments showed a mixture of INA form III and form II, while the XRPD pattern of the 10 kV experiment only displayed INA form II. Experiments performed in the absence of the electric field yielded form III. Appendix H displays the corresponding XRPD patterns. It can be concluded that the polymorphic structure changes from the metastable form III to the stable form II with increasing values of the electric field strength. This phenomenon was also observed in the Crystalline setup, but there the electric field strength was insufficient to obtain (only) the stable polymorph. The change in polymorphic outcome (from a metastable to the stable form) can be attributed to the fact that the electric field affects the orientation of the solute molecules in solution in such a way that they are more aligned. It can be stated that with increasing electric field strengths more solute molecules are aligned, so that at a certain field strength only one specific polymorph is obtained. The electric field strength necessary to obtain the stable polymorph is $5.7 \cdot 10^5$ V $m^{-1}$. This result showed that a change in polymorphic outcome occurred under influence of increasing electric field strengths and confirms that the polymorphic outcome of a cooling crystallization experiment is affected by the electric field. In future work, this result could be applied for polymorphic control in crystallization processes (e.g. in the pharmaceutical industry).

X-ray powder diffraction determined besides the crystal structure also the crystalline and amorphous fraction of the acquired crystals. It was observed that the crystalline fraction showed a decrease upon increasing field strengths, which can be seen in table 2. This is an unexpected result, because one would expect an ordered crystalline phase due to the alignment of solute molecules. A possible explanation for this trend is that the electric field has an effect on the crystal growth rate. One could imagine that due to a higher crystal growth rate, the time for a solute molecule to diffuse and incorporate into the crystal lattice is insufficient to obtain an ordered crystalline structure which enhances the amorphous fraction. It must be emphasized that this is a possible explanation and that the electric field effect on crystal growth was not studied in this thesis. Also it must be noted that this specific measurement technique is not very accurate to determine the crystalline fraction, but it gives an indication of the crystalline and amorphous fractions.

Table 2: Crystalline and amorphous fractions of experiments conducted at different potential differences.

| Experiment | Crystalline [%] | Amorphous [%] |
|---|---|---|
| Manufacturer | 89 | 11 |
| 0 kV | 85 | 15 |
| 5 kV | 87 | 13 |
| 7.5 kV | 82 | 18 |
| 10 kV | 78 | 22 |

Also in this experimental setup the crystals grew primarily on the anode, which is depicted in figure 19. There were no visible crystals at other locations, which is explained by the fact that the electric field can induce a dipole moment. The anode attracts the negatively charged compound so that convection occurs and locally a concentration gradient exists. In this way crystallization could occur only on the anode.

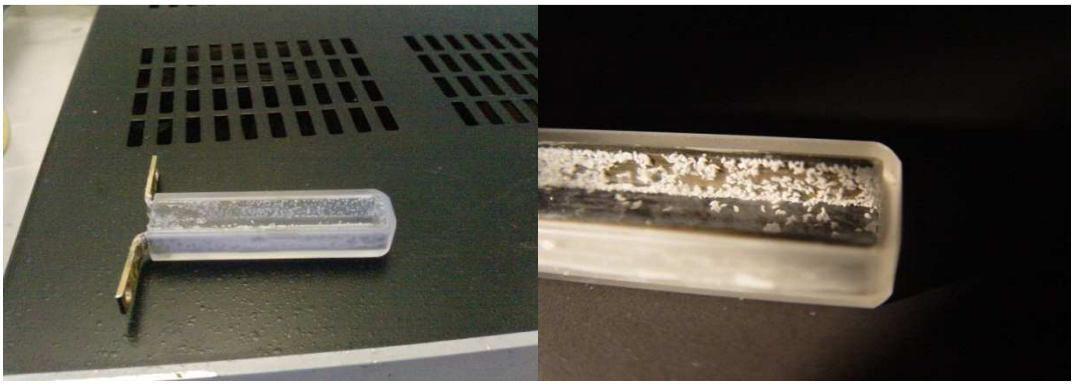

Figure 19: Pictures of the crystal formation on the electrodes of the parallel-plate setup. It is seen that on one specific electrode (anode) more crystals are formed.

In table 3 the results obtained in the parallel-plate setup are summarized. The mean particle size is approximated via micrographs obtained with the optical and scanning electron microscope. A scale bar was used to check the particle sizes, so it must be noted that this measuring technique is not the most accurate technique available.

Table 3: Summarization of the obtained results in the presence of an electric field.

| C = 35 mg $mL^{-1}$ | Potential difference [kV] | | | |
|---|---|---|---|---|
| | 0 | 5 | 7.5 | 10 |
| Nucleation | Throughout | Anode | Anode | Anode |
| Polymorphic outcome | Form III | Form II, Form III | Form II, Form III | Form II |
| Crystalline fraction | 89 | 85 | 82 | 78 |
| Mean particle size [µm] | 550 | 200 | 350 | 350 |

Figure 20 represents the optical micrographs of the INA crystals obtained from the +5 kV experiment and figure 21 gives the optical micrographs from the +10 kV experiment. Next the scanning electronmicrographs are given for both experiments in figures 22 and 23. The optical micrographs show that the crystals have an elongated rhombic shape.

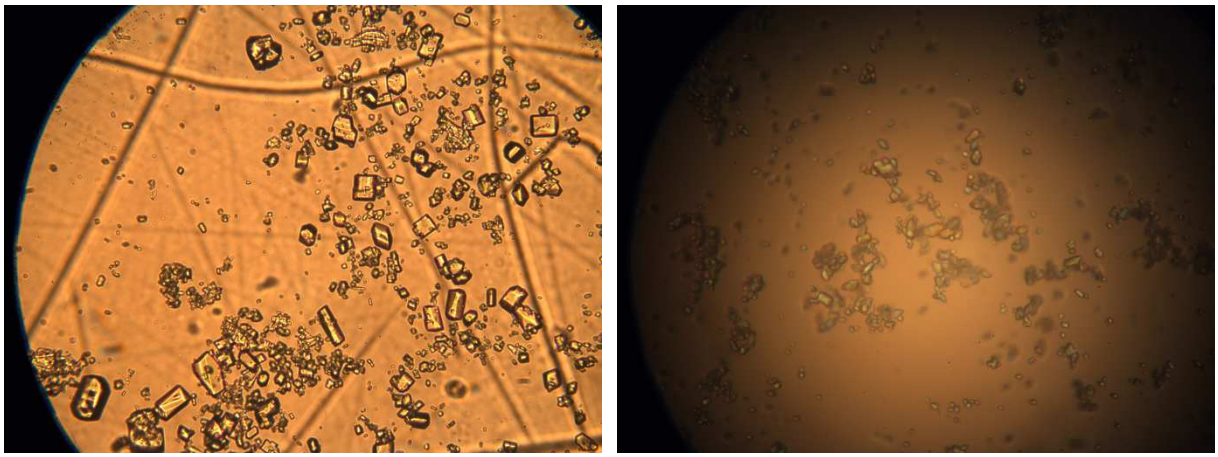

Figure 20: Optical images of INA crystals obtained from a +5 kV experiment. Magnification 20x (left) and 50x (right).

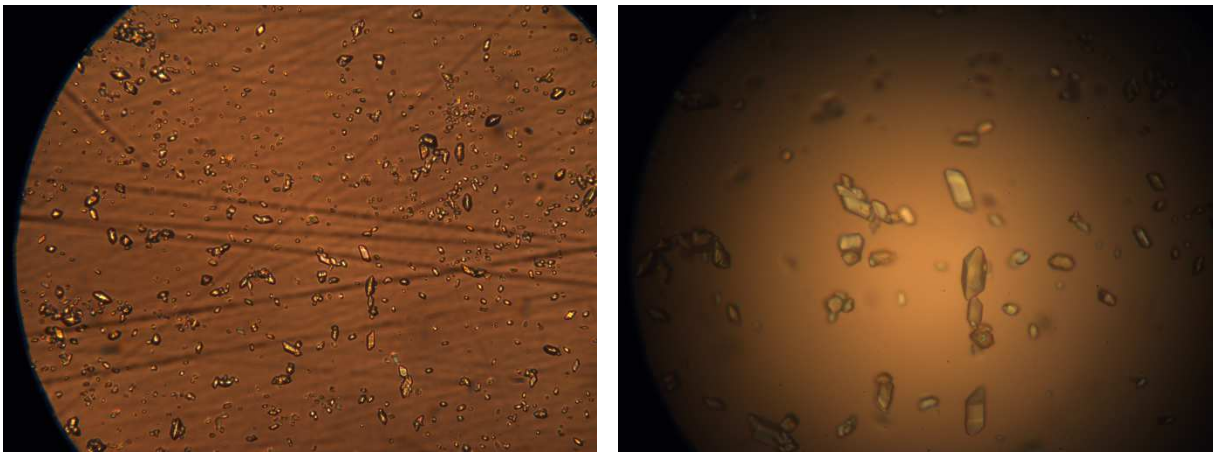

Figure 21: Optical images of INA crystals obtained from a +10 kV experiment. Magnification 20x (left) and 50x (right).

The scanning electromicrographs show that the amount of crystals produced in a + 5 kV experiment is bigger than in a +10 kV experiment, but that the crystals are relatively smaller. The mean particle size in a +5 kV experiment is 200 µm and in a +10 kV experiment 350 µm. Furthermore, one can see that a fraction of the crystals has an amorphous phase and that small fragments are present due to attrition, filtration or scraping crystals of the electrodes.

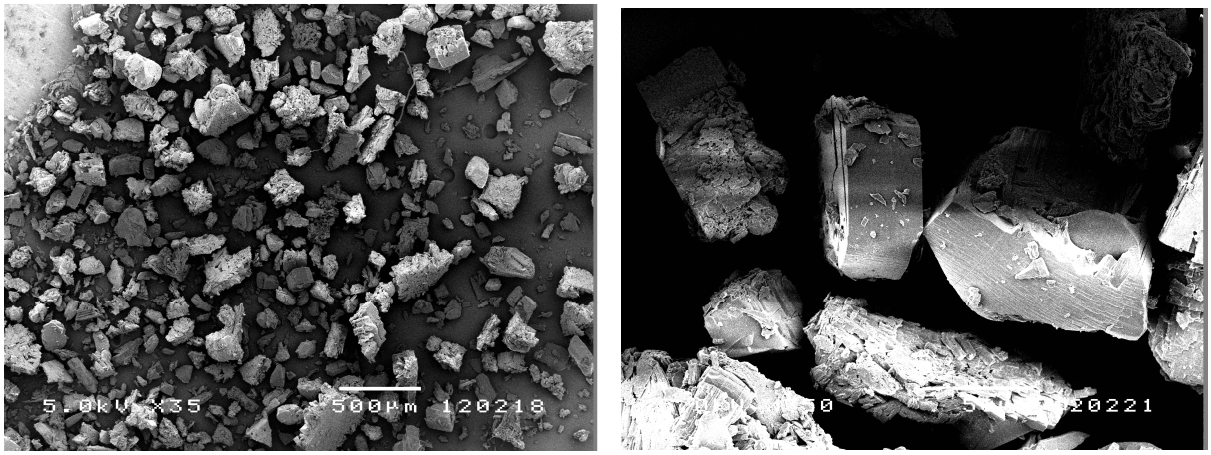


Figure 22: Scanning electronmicrographs of INA crystals obtained from a +5 kV experiment.

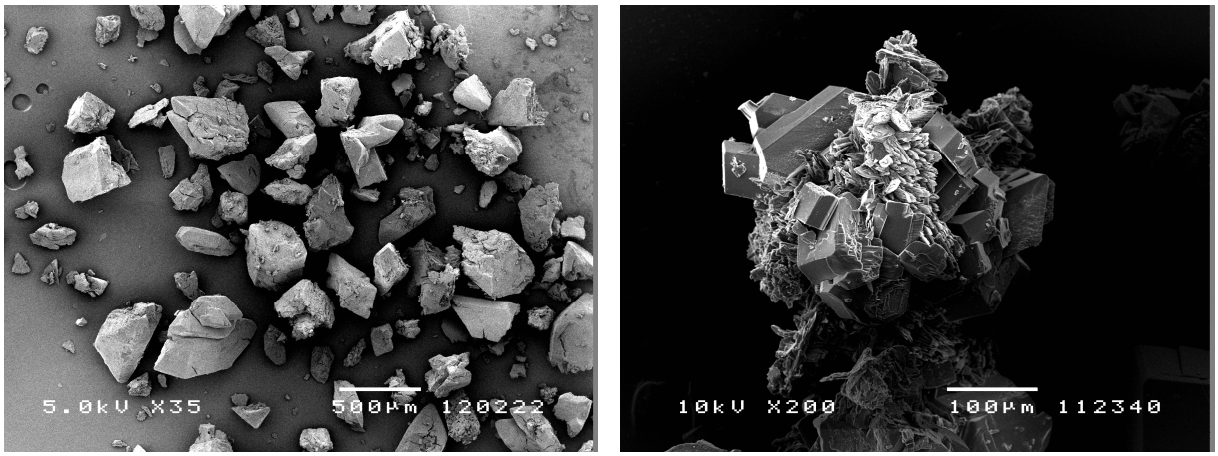


Figure 23: Scanning electronmicrographs of INA crystals obtained from a +5 kV experiment.

## 4.5 Induction time

### 4.5.1 Induction time in the absence of the electric field

Induction time measurements of INA in 1,4-dioxane were performed at supersaturation ratios 1.47, 1.76, and 2.05. At S = 1.47 128 identical induction time measurements were conducted in 1 ml samples at 25 °C. This many measurements were taken, because this supersaturation ratio lies within the metastable region where no spontaneous nucleation occurs. At the other supersaturation ratios 64 identical experiments were taken in 1 ml samples at 25 °C. The first ratio lies precisely on the metastable zone limit and the last ratio lies above the metastable zone limit in the nucleation region. Appendix J shows the induction time results at each supersaturation. Induction times showed, as expected, a large variation at a certain supersaturation. For instance, at S = 1.76, the induction time varied from 2 to 71 minutes. At relatively small volume and low supersaturation the probability that nuclei form in solution is low, which leads to a large variation in induction time. This large variation reflects the statistical nature of nucleation.[27]

Induction time can be defined as the period of time between the achievement of supersaturation and the detection of crystals. The induction time probability *P(t)* gives the chance that for certain conditions at a specific time crystals are detected. This can be determined from a large number of induction time experiments at constant supersaturation, temperature, and volume. For *N* isolated experiments, the probability that crystals are detected at time *t* is given by

$$P(t) = \frac{N^{+}(t)}{N} \qquad \textbf{(4-1)}$$

where $N^{+}(t)$ is the number of experiments in which crystals are detected at time *t*. The *P(t)* is plotted versus induction time for each supersaturation ratio, which is shown in figure 24.[22]

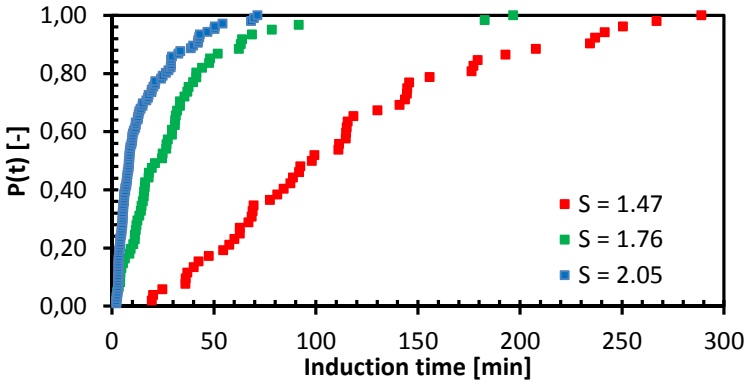


**Figure 24: Induction time probability versus induction time for three different supersaturation ratios; S = 1.47 (red line), 1.76 (green line), and 2.05 (blue line).**

Figure 24 shows that for increasing supersaturation ratios, the induction time decreases. The range of variation in induction time becomes less with increasing supersaturation ratio. All this indicates that a high nucleation rate is present in systems with high supersaturation. For instance, at S = 1.47 after 100 minutes 50% of the sample was crystallized. At S = 1.76 and 2.05 the same level was reached in 20 and 8 minutes, respectively. Induction time measurements were important for this research, because it is essential to know when nucleation starts in the system. The electric field must be present when nucleation starts in order to see an effect on the outcome of the crystallization process. This effect could be on the alignment of solute molecules and hence the frequency factor and nucleation rate or could have an effect on the nucleation work. Thus, from these experiments an estimation can be made when to apply the electric field during the crystallization process. It was chosen not to apply the electric field initially in order to prevent distortion of the solvent structure.

### 4.5.2. Induction time in the presence of the electric field

Induction time measurements of INA in 1,4-dioxane in the presence of the electric field (± $10^5$ V $m^{-1}$) were performed at a supersaturation ratio of 2.05. At this supersaturation ratio 20 identical induction time measurements were conducted in the Crystalline for 4 mL samples. This many measurements were taken to get representative results. These results are compared to the results obtained at the same supersaturation ratio in the absence of the electric field, which is shown in figure 25.

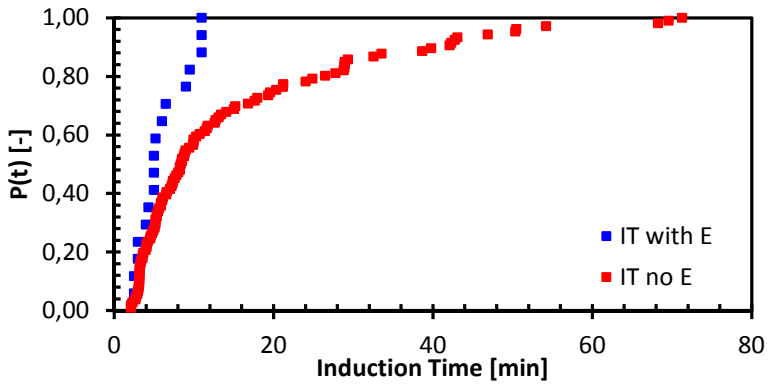


**Figure 25: Induction time probability versus induction time at a supersaturation ratio of 2.05 measured in the absence of an electric field (red line) and in the presence of an electric field (blue line)**

It must be noted when comparing these results that the experiments performed without the electric field were done in the Crystal16 and in 1 mL vials, whereas the experiments conducted under the influence of an electric field were done in the Crystalline and in 4 mL vials. So care must be taken in order to be conclusive about the electric field effect on the induction time of a cooling crystallization process. It is observed that the induction time is less in the presence of the electric field (80% is crystallized in 10 minutes), than in the absence of the electric field (80% is crystallized in 27 minutes). It seems that the electric field had an effect on the crystallization process by lowering the nucleation work for crystal formation, which lead to a decrease in induction time. The Gibbs free energy for crystal formation could be lowered, so that this energy barrier (eq. **2-4**) is more easily overcome. This could happen if the dielectric constant of the solution exceeds the dielectric constant of the crystalline phase.

# 5. Conclusions and recommendations

The main goal of this research was to investigate and understand the effect of a strong DC electric field on crystal nucleation and polymorphic outcome in a cooling crystallization process. Two experimental setups were built in order to examine this effect. The Crystalline multiple reactor station equipped with an on-board camera and Raman spectrometer was used to perform *in situ* measurements during cooling crystallization. A parallel-plate setup was used to create a more or less homogeneous electric field ($\pm 10^5$ V $m^{-1}$) and provided a method to investigate the polymorphic outcome.

Material selection was important, because crystallization in the presence of an electric field imposes different requirements on the system and its compounds. The solute must have the favorable properties of a high dipole moment and a distinct polymorphic shape. Compounds isonicotinamide and 4-hydroxybenzoic acid were suitable for this study, because they possessed these qualities. Isonicotinamide has a dipole moment of 3.56 D and there are six known polymorphs. The stable polymorph has a dimer structure, whereas the metastable forms have a chain-like structure. 4-Hydroxybenzoic acid has a dipole moment of 3.35 D and has two known polymorphs. The stable form has a dimer structure and the metastable polymorph has a chain-like structure. Solvent selection was based on interaction with the electric field and in order to reduce this interaction the solvent must possess a low dielectric constant and dipole moment. The non-polar solvent 1,4 dioxane was preferred due to its favorable dielectric properties. In conclusion, great care was taken to choose materials that are suitable for crystallization under the influence of a DC electric field.

An essential step in understanding the crystallization behavior and conducting experiments is the characterization of materials. That is the reason that solubility and metastable zone width of both model compounds in 1,4-dioxane were measured. The obtained solubility curves were very temperature dependent, which suggests that cooling crystallization is the best crystallization technique for these polymorphic systems.

The Crystalline multiple reactor system performed experiments in the absence as well as in the presence of a strong DC electric field ($\pm 10^5$ V $m^{-1}$) to investigate the electric field effect on the cooling crystallization process. In these experiments it was observed that the polymorphic outcome has changed from one polymorphic form to another. In the case of isonicotinamide it was observed that the polymorphic outcome changes from purely a metastable form (in the absence of the electric field) to a mixture of the stable form II and metastable form I (in the presence of the electric field). Experiments performed with 4-hydroxybenzoic acid showed that the purchased stable form recrystallized in the absence of the electric field to a mixture of both the stable and metastable form. Under the influence of a strong DC electric field only the metastable polymorph was obtained. This difference in polymorphic outcome is explained by the fact that a strong DC electric field affects the orientation of solute molecules in solution. Due to the presence of an electric field, solute molecules in solution are more aligned than in the absence of an electric field. The alignment of solute molecules causes that one specific polymorphic form is preferred or energetically favorable over the other polymorphic forms. When the molecules are more aligned one could imagine that the number of effective collisions (frequency factor) and thereby the nucleation rate would increase, which enhances the formation of one specific polymorph.

Next the *in situ* solution Raman spectra showed no polymorphic transition. The main reason is that crystal formation took place on the electrodes and not within the solution. The Raman laser was directed to the middle of the solution (between the electrodes) and so the produced crystals on the electrodes were not detected by the Raman laser. Another interesting finding was that crystallization occurred in the presence of the electric field only on the electrodes (mainly the anode). This observation can be explained by the fact that the electric field can induce a dipole moment. The anode attracts the negatively charged compound so that convection takes place and locally a concentration gradient exists. In this manner crystallization occurred only on the anode.

Finally, it was observed that the induction time is less in the presence of the electric field (80% is crystallized in 10 minutes), than in the absence of the electric field (80% is crystallized in 27 minutes). A possible explanation for this effect is that the electric field affects the crystallization process by lowering the nucleation work for crystal formation, which lead to a decrease in induction time.

The parallel-plate setup performed experiments with model compound isonicotinamide at different potential differences (+5, +7.5, and +10 kV). In the absence of the electric field metastable form III was obtained. At +5 and +7.5 kV a mixture of both the stable polymorph and the metastable form III was produced and at +10 kV only the stable polymorphic form II was acquired. So the polymorphic outcome changed from purely metastable form III to purely the stable form II. This effect was also observed in the Crystalline setup, but there the electric field strength was insufficient to obtain (only) the stable polymorph. This change in polymorphic outcome can be attributed to the fact that the electric field affects the orientation of the solute molecules in solution in such a way that they are more aligned, which enhances the formation of one specific polymorph. It can be concluded that with increasing electric field strengths more solute molecules are aligned, which causes that one specific polymorph is obtained. The electric field strength necessary to obtain the stable polymorph is around $5.7 \cdot 10^5$ V $m^{-1}$. This result showed that a polymorphic transition occurred under influence of increasing electric field strengths and confirms that the polymorphic outcome of a cooling crystallization experiment is affected by the electric field. This result may in the future, for instance, be used in the pharmaceutical industry in order to control the polymorphic outcome of a cooling crystallization process.

Future research should focus on doing more cooling crystallization experiments with and without the electric field present in the Crystalline setup. This would apply for both model compounds, but especially for 4-hydroxybenzoic acid because that is a very promising compound and until now few experiments have been performed. One could do experiments at different concentrations, cooling rates, and electric field strengths to further investigate the influence of an electric field on the crystallization process. Also for both model compounds the electric field effect on the induction time should be measured and many experiments should be executed in the same experimental setup and in the absence and in the presence of the electric field to obtain representative results. Next to nucleation, polymorphic outcome, and induction time one shall check the effect of the electric field on crystal formation, growth, and crystal size. Furthermore, new compounds (e.g. pharmaceutical compounds) and solvents could be used in order to obtain extensive results on the electric field effect on different polymorphic systems. Also more discussion is needed to connect the theoretical background with the observations seen during experiments. Finally, it would be advantageous to model the electric field strength within the confined space of the Crystalline reactor in order to understand which field strength is necessary to measure an effect.

# References


[1] Jiang, S., *Crystallization Kinetics in Polymorphic Organic Compounds*, Delft University of Technology, Delft, **2009**, 3 – 9.

[2] Caira, M.R., *Crystalline Polymorphism of Organic Compounds*, Cape Town, **1998**, 164 – 176.

[3] Kramer, H.J.M.; Van Rosmalen, G.M.; Ter Horst, J.H., *Basic Process Design for Crystallization Processes*, Delft University of Technology, Delft, 6 – 34.

[4] Kashchiev, D., *Journal of Crystal Growth*, **1972**, 13-14, 128 – 130.

[5] Saban, K.V.; Thomas, J.; Varughese, P.A.; Varghese, G., *Crystal Research and Technology*, **2002**, 11, 1188 – 1199.

[6] Ziabicki, A.; Jarecki, L., *Crystal nucleation in an electric field*, **1996**, Macro. Symp. 104, 65 – 87.

[7] Hammadi, Z.; Astier, J.P.; Morin, R.; Veesler, S., *Crystal Growth & Design*, **2009**, 9, 3346 – 3347.

[8] Hammadi, Z.; Veesler, S., *Biophysics and Molecular Biology*, **2009**, 101, 38 – 44.

[9] Moreno, A.; Sazaki, G., *Journal of Crystal Growth*, **2004**, 264, 438 – 444.

[10] Nogueira, E.M. et al., *Solid state sciences*, **2001**, 3, 733 – 740.

[11] McCrone, W.C.; Fox, D.; Labes, M.M.; Weissberger, A., *Physics and Chemistry of the organic solid state*, Eds. Wiley Interscience, New York, **1965**, Vol. 2, 725 – 767.

[12] Mullin, J.W., *Crystallization*, 4th ed., Butterworths, London, **2001**.

[13] Kitamura, M., *Crystal Engineering Communications*, **2009**, 11, 949 – 964.

[14] Seader, J.D.; Henley, E.J., *Separation Process Principles*, 2nd ed., John Wiley & Sons, Inc, New York, **2006**, Ch. 17 644 – 690.

[15] Yu, L.X. et al., *Advanced Drug Delivery*, **2003**, 350 – 368.

[16] Van der Graaf, J., *Sonocrystallization*, MSc. Thesis, Delft University of Technology, **2011**, 2 – 5.

[17] Aakeröy, C.B.; Beatty, A.M.; Helfrich, B.A., Nieuwenhuyzen, M., *Crystal Growth &Design*, **2003**, 3, 159 – 165.

[18] Li, J.; Bourne, S.A.; Caira, M.R., *Chem. Comm.*, **2011**, 47, 1530 – 1532.

[19] Eccles, K.S.; Deasy, R.E.; Fabian, L.; Braun, D.E.; Maguire, A.R.; Lawrence, S.E., *CrystEngComm*, **2011**, 13, 6923 – 6925.

[20] http://www.avantium.com, **06-04-12**.

[21] Gaincoli, D.C., *Physics for scientists & engineers*, 3rd ed., Prentice Hall, New Jersey, **2000**

[22] Jiang, S., *Crystallization Kinetics in Polymorphic Organic Compounds*, Delft University of Technology, Delft, **2009**, 100 – 109.

[23] Prasad, A.I., *Isonicotinamide complexes with some metal(II) halides and pseudohalides*, Inorganic and Nuclear Chemistry Letters, **1976**, 12, pg. 777.

[24] Zhang, Y.; Chang, A.; Wang, ?.; Kim, ?.; Morris, N., *Electric field directed growth of aligned single walled carbon nanotubes*, Applied Physics Letters, **2001**, 79, pg. 3155 – 3157.

[25] Smith, P.A.; Nordquist, C.D.; Jackson, T.N.; Martin, B.R., *Electric field assisted assembly and alignment of metallic nanowires*, Applied Physics Letters, **2000**, 77, pg. 1399 – 1401.

[26] Kulkarni, S.A.; McGarrity, E.S.; Meekes, H.; ter Horst, J.H., *Isonicotinamide self-association: the link between solvent and polymorph nucleation*, ChemComm, **2012**, 48, pg. 4983 – 4985.

[27] Kulkarni, S.A.; Kadam, S.S; Meekes, H.; ter Horst, J.H., *Easy access to valuable industrial nucleation kinetics*, TU Delft and Radboud universtiteit Nijmegen.

# List of symbols

## Latin capitol

| Abbreviation | Explanation | Value | Units |
|---|---|---|---|
| A | Pre-exponential factor | | - |
| E | Electric field strength | | $V\ m^{-1}$ |
| $\Delta G$ | Total Gibbs free energy | | J |
| $\Delta G^*$ | Gibbs free energy to create a nucleus | | J |
| $\Delta G_E$ | Electric field Gibbs free energy contribution | | J |
| J | Nucleation rate | | $\#nuclei\ m^{-3}\ s^{-1}$ |
| R | Universal gas constant | 8.314 | $J\ mol^{-1}\ K^{-1}$ |
| S | Supersaturation ratio | | - |
| T | Temperature | | K |
| $T_S$ | Standard temperature | 273.15 | K |

## Latin non-capitol

| Abbreviation | Explanation | Value | Units |
|---|---|---|---|
| c | Concentration | | $kg\ m^{-3}$ |
| $c^*$ | Equilibrium concentration | | $kg\ m^{-3}$ |
| $k_b$ | Boltzmann constant | $1.38 \cdot 10^{-23}$ | $J\ K^{-1}$ |
| $p_S$ | Standard pressure | $1.01325 \cdot 10^5$ | Pa |
| r | Sphere radius | | m |
| $r^*$ | Critical nucleus radius | | m |
| x | Number of molecules in cluster | | - |

## Greek non-capitol

| Abbreviation | Explanation | Value | Units |
|---|---|---|---|
| $\gamma$ | Interfacial tension | | $N\ m^{-1}$ |
| $\gamma_a$ | Activity coefficient | | - |
| $\varepsilon_c$ | Dielectric constant crystalline phase | | - |
| $\varepsilon_s$ | Dielectric constant solid phase | | - |
| $\Delta\mu$ | Chemical potential difference | | $J\ mol^{-1}$ |
| $\mu_s$ | Chemical potential solid phase | | $J\ mol^{-1}$ |
| $\mu_c$ | Chemical potential crystalline phase | | $J\ mol^{-1}$ |
| $\pi$ | Pi | 3.1415 | - |
| $\sigma$ | Relative supersaturation | | - |
| $\psi$ | Constant appearing in $\Delta G_E$ | | - |
| $\omega$ | Molecular volume | | $m^3\ mol^{-1}$ |

# Acknowledgements

This research was done under the supervision of N. Radacsi and Dr. Ir. J.H. ter Horst. Experiments were performed in the lab at the Process & Energy building, Leeghwaterstraat 44, Delft, The Netherlands. I want to thank Norbert Radacsi, Samir Kulkarni and Joop ter Horst for their stimulating and fruitful discussions. Furthermore, I would like to thank Michel van den Brink for his help in the laboratory, Ruud Hendrikx for measuring the x-ray powder diffraction patterns, and Piet Droppert for DSC and TGA analysis. Avantium Technologies is acknowledged for their support.

# Appendix

## Appendix A Nucleation

There are two distinct mechanisms for crystal nucleation namely primary and secondary nucleation (attrition). Primary nucleation is the crystal creation within a supersaturated solution and it can be divided into homogeneous and heterogeneous nucleation. The formation of crystals from a clear supersaturated solution is known as homogeneous nucleation, while heterogeneous nucleation is known as the formation of crystals on foreign substances (e.g. seeds, reactor wall, dust).

Nucleation is a two-step process where first the formation of small clusters of solute molecules takes place followed by an organizational step in which the cluster takes on a crystalline structure. Consider the energy involved in solid phase formation and in creation of the surface of a spherical cluster of molecules in a supersaturated fluid. The Gibbs free energy required for the formation of a crystalline cluster in a supersaturated solution is given by

$$\Delta G = 4\pi r^2 \gamma - x k_B T \ln S$$

where $r$ is the sphere radius, $k_b$ is the Boltzmann constant, S is the supersaturation ratio, and $\gamma$ is the interfacial tension. The first and second term represent the surface- and volume energy, respectively, in the classical nucleation theory.

To determine the radius of the critical nucleus the total $\Delta G$ must be minimized with respect to $r$. Any crystal smaller than the critical nucleus is unstable and tends to dissolve. The critical radius $r^*$ is given by

$$r^* = \frac{2\gamma\omega}{k_B T \ln S}$$

So its size depends on supersaturation, interfacial energy, and the molecular volume. Clusters with radii exceeding the critical nucleus are stable and have the tendency to grow to macroscopic size. The Gibbs free energy needed to create a nucleus can be determined by combining the equations

$$\Delta G^* = \frac{16\pi\ \gamma^3 \omega^2}{3\left[k_B T \ln S\right]^2}$$

where $\omega$ is the molecular volume, and $\Delta G^*$ is the nucleation work. This is an energy barrier for nucleation to occur.

Homogeneous nucleation can only occur if this energy barrier is overcome. The time it takes for homogeneous nucleation to happen is called the induction time. It is defined as the period of time between the achievement of supersaturation and the detection of crystals. With increasing supersaturation, the energy barrier is decreased and so as a result the induction time decreases with increasing supersaturation. With the use of the nucleation work one can obtain the nucleation rate

$$J = A\exp\left(-\frac{\Delta G^*}{k_B T}\right)$$

where *A* is a pre-exponential factor. The nucleation rate for homogeneous nucleation is expressed in number of nuclei per unit of volume per unit of time.

Heterogeneous nucleation happens in the presence of foreign substances, because a phase boundary or impurity lowers the free energy needed to reach the critical nucleus size. The reason for this is that the activation energy for nucleation work is lowered when nuclei form on preexisting surfaces or interfaces, since the surface tension is reduced. In other words, it is easier for nucleation to occur at surfaces and interfaces than from solution. Therefore, heterogeneous nucleation occurs more readily than homogeneous nucleation and is responsible for the majority of primary nucleation in crystallization processes.[1] The Gibbs free energy needed for heterogeneous nucleation is equal to the product of homogeneous nucleation and a function of the contact angle

$$\Delta G_{het} = \Delta G_{\text{hom}} \cdot f(\theta)$$

$$f(\theta) = \frac{1}{2} - \frac{3}{4}\cos(\theta) + \frac{1}{4}\cos^3(\theta)$$

So it can be concluded that heterogeneous nucleation takes place on preferential sites due to an lower effective surface energy and so it requires less energy than homogeneous nucleation. The wetting angle in fact determines the ease of nucleation by reducing the energy needed.

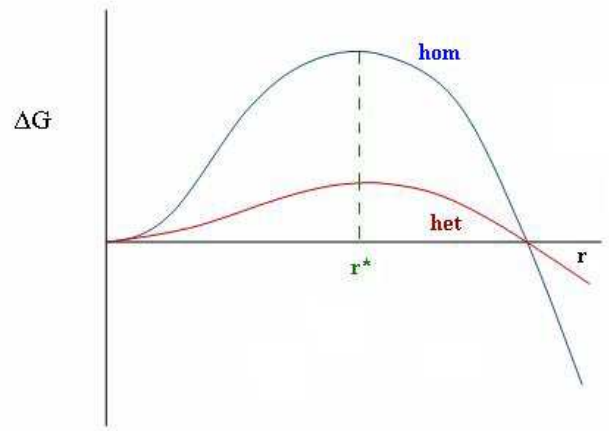


**Figure 26: The Gibbs free energy difference between homogeneous and heterogeneous nucleation.[2]**

Secondary nucleation is the formation of new crystals in the presence of existing crystals. This type of crystallization can be attributed to fluid shear or to collisions between already existing crystals with either a solid surface (e.g. agitator) or with each other. Attrition is the dominant form of nucleation in industrial crystallization processes.

[1] Kramer, H.J.M.; Van Rosmalen, G.M.; Ter Horst, J.H., *Basic Process Design for Crystallization Processes*, Delft University of Technology, Delft, 6 – 34.
[2] William, D.; Callister, Jr., *Materials science and engineering an introduction*, John Wiley & Sons, Inc., 7, **2007**

# Appendix B Basic physics[3]

## B.1 Electric potential

Electric potential is defined as electric potential energy per unit charge. That is, the electric potential difference between any two points in space is defined as the difference in potential energy of a charge q placed at those two points, divided by the charge q

$$\Delta V = \frac{U_b - U_a}{q}$$

Potential difference is measured in volts (1 V = 1 J $C^{-1}$) and is sometimes referred to as voltage. Thus, electric potential difference is a measure of how much energy an electric charge can acquire in a given situation. And, since energy is the ability to do work, the electric potential difference is also a measure of how much work a given charge can do. The change in potential energy of a charge when it moves through a potential difference is

$$\Delta U = q \cdot \Delta V$$

The effects of any charge distribution can be described either in terms of electric field or in terms of electric potential. Electric potential is often easier to use because it is a scalar, as compared to electric field which is a vector. There is a crucial connection between the electric potential produced by a given arrangement of charges and the electric field due to those charges. The relation between a conservative force F and the potential energy U associated with that force is given by

$$\Delta U = -\int F \cdot dl$$

In the electric case one is more interested in potential difference. Then the potential difference between two points is given by the following relation

$$\Delta V = -\int E \cdot dl$$

Thus, ΔV can be found in any region where E is known. When the field is uniform it is easy to solve and when V is known, the components of E can be found from the from the following equation

$$E = -\frac{dV}{dl}$$

An equipotential line or surface is all at the same potential, and is perpendicular to the electric field at all points. There can be no electric field within a conductor in the static case, or otherwise the free electrons would feel a force and would move. Indeed, the entire volume of a conductor must be entirely at the same potential in the static case, and the surface of a conductor is then an equipotential surface. The electric potential due to a single point charge Q, relative to zero potential at infinity, is given by

[3] Gaincoli, D.C., *Physics for scientists & engineers*, 3rd ed., Prentice Hall, New Jersey, **2000**

$$V = \frac{1}{4\pi\varepsilon_0}\frac{Q}{r}$$

The potential due to any charge distribution can be obtained by summing over the potentials for all charges. Two equal point charges Q, of opposite sign, separated by a distance l, are called an electric dipole. The electric potential at an arbitrary point due to a dipole is given by the sum of both potentials due to each of the two charges.

$$V = \frac{1}{4\pi\varepsilon_0}\frac{Q}{r} + \frac{1}{4\pi\varepsilon_0}\frac{-Q}{r+\Delta r} = \frac{Q}{4\pi\varepsilon_0}\frac{\Delta r}{r\left(r+\Delta r\right)}$$

Where r is the distance from a point to the positive charge and r + Δr the distance from point P to the negative charge. Now assume that the distance to point P is much larger than the distance between the two charges, r >> l. Then one can say Δr = l·cos(θ). Since r >> Δr one can neglect it in the denominator. Then the following equation is obtained.

$$V = \frac{1}{4\pi\varepsilon_0}\frac{Ql\cos\left(\theta\right)}{r^2} = \frac{1}{4\pi\varepsilon_0}\frac{p\cos\left(\theta\right)}{r^2}$$

Here p = Q·l is called the dipole moment. When θ is between 0-90, then V is positive, otherwise it is negative. From this equation it can be seen that the potential decreases as the square of the distance from the dipole, whereas for a single point charge the potential decreases with the first power of the distance.

## B.2 Capacitor

A capacitor is a device used to store charge and consists of two separated conductors. The two conducting plates are placed near each other but not touching. A simple capacitor consists of a pair of parallel plates separated by a small distance. Often the two plates are rolled into the form of a cylinder with paper or other insulator separating the plates. The two conductors generally carry equal and opposite charges and the ratio of this charge to the potential difference between the conductors is called the capacitance

$$Q = C \cdot \Delta V$$

The unit of the capacitance is farad (F = C $V^{-1}$). The capacitance does not in general depend on Q or V, but its value depends only on the size, shape, and relative position of the two conductors, and also on the material that separates them. For the example of two separate plates one knows that the electric field has magnitude

$$E = \frac{Q}{\varepsilon_0 \cdot A}$$

The relation between electric field and electric potential results in the following relation

$$\Delta V = \frac{Qd}{\varepsilon_0 A}$$

The capacitance of a parallel-plate capacitor is proportional to the area of each plate and inversely proportional to their separation

$$C = \varepsilon_0 \frac{A}{d}$$

The space between the conductors contains a non-conducting material such as air, paper or plastic. The latter materials are referred to as dielectrics, and the capacitance is proportional to a property of the dielectric called the dielectric constant, K (nearly 1 for air). For a parallel-plate capacitor

$$C = K\varepsilon_0 \frac{A}{d} = \varepsilon \frac{A}{d}$$

Where ε is called the permittivity and $\varepsilon_0$ is called the permittivity of vacuum.

In most capacitors there is an insulating sheet of material (e.g. paper, plastic etc.) called a dielectric between the plates. This serves several purposes. First of all, dielectrics break down (allowing electric charge to flow) less readily than air, so higher voltages can be applied without charge passing across the gap. Furthermore, a dielectric allows the plates to be placed closer together without touching, thus allowing an increased capacitance because the distance is less. Finally it is found experimentally that if the dielectric fills the space between the two conductors, it increases the capacitance by a factor K which is known as the dielectric constant. So $C = KC_0$, where $C_0$ is the capacitance when the space is a vacuum and C is the capacitance when the space is filled with a material whose dielectric constant is K.

# Appendix C Photos of the Crystalline multiple reactor station setup

This section gives actual photos of the Crystalline experimental setup.

**Figure 27: Front and side view of the Crystalline experimental setup. In the middle stands the Crystalline multiple reactor station and on the left the Raman spectroscope is coupled. The power supply is situated on the right.**

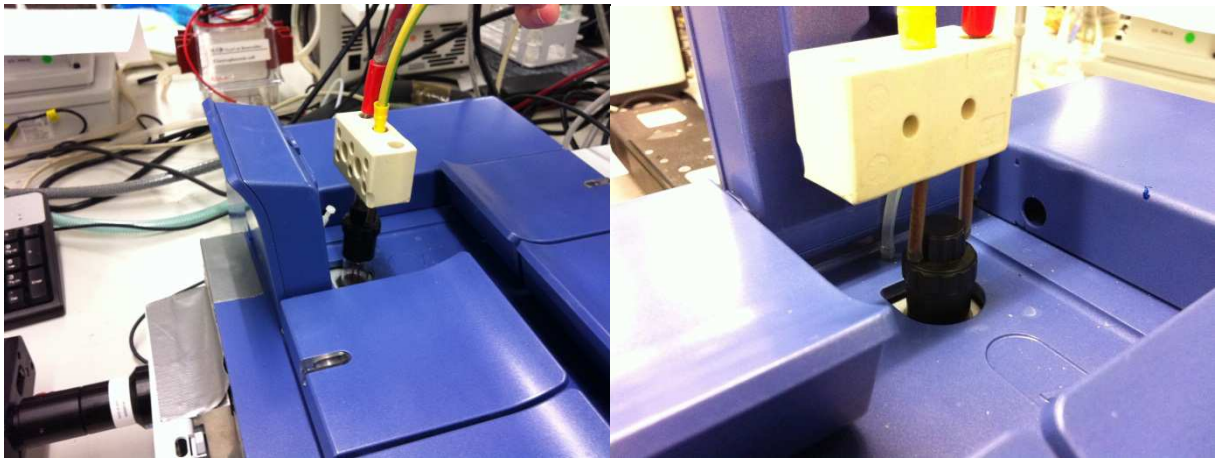

**Figure 28: A 8 mL disposable vial with a cap which includes the electrodes. A connector block is used to connect the electrodes (copper wires) to the high voltage cable. The vial is placed in one of the reactors of the Crystalline.**

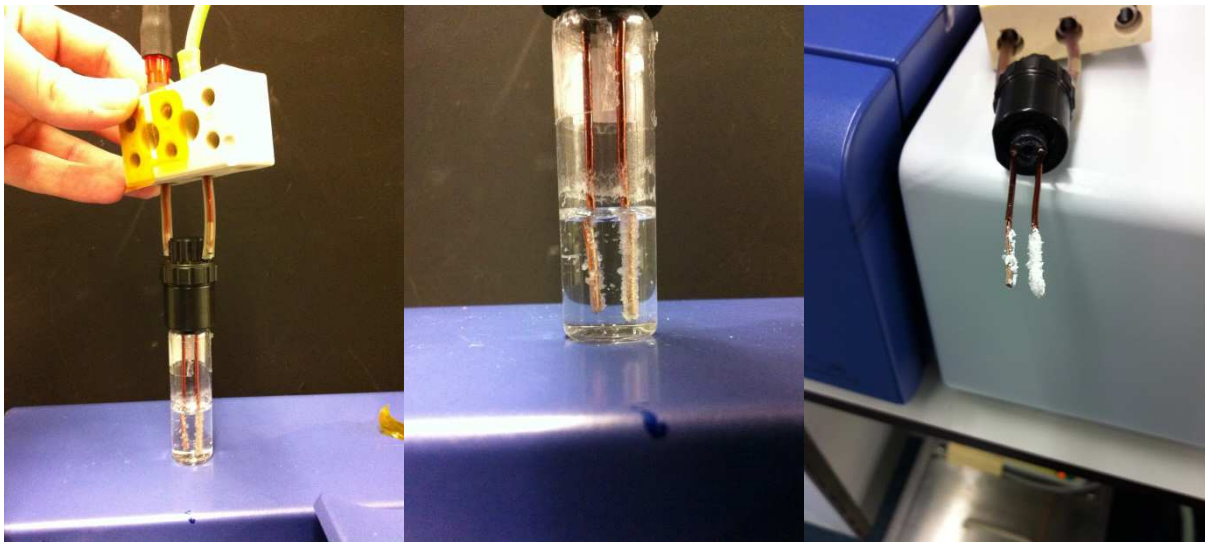

**Figure 29: Crystals obtained mainly on the anode after a cooling crystallization experiment.**

# Appendix D Photos of the parallel-plate setup

This section gives actual photos of the experimental setup


**Figure 30: The parallel-plate setup is located in the middle and a small beaker is used to hold the setup steady. A high voltage power supply is located at the right. Artificial light was used to made observations in the setup.**

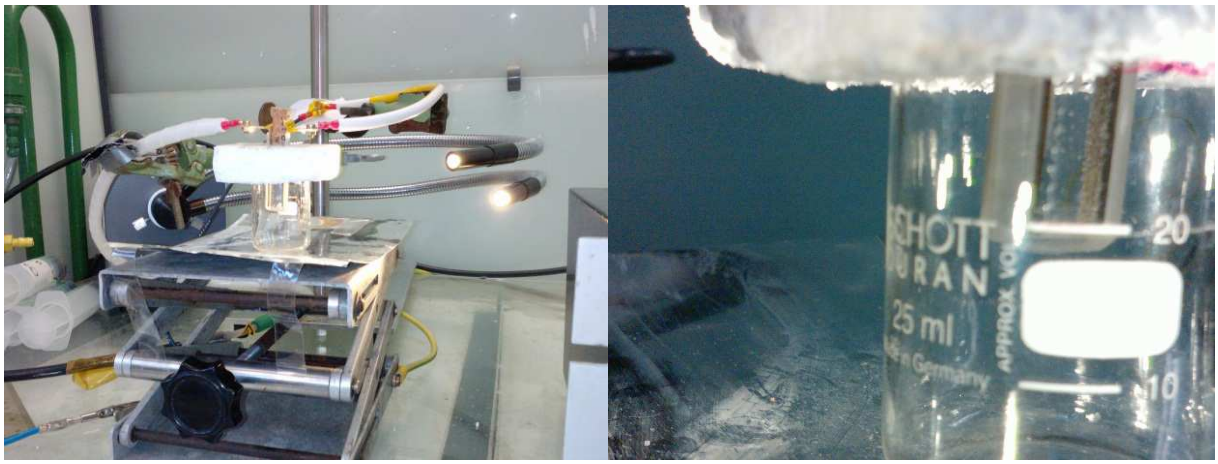


**Figure 31: The parallel-plate setup. High voltages cable were connected to the electrodes via a screw and a bolt. The right picture shows crystal formation during an cooling crystallization experiment.**

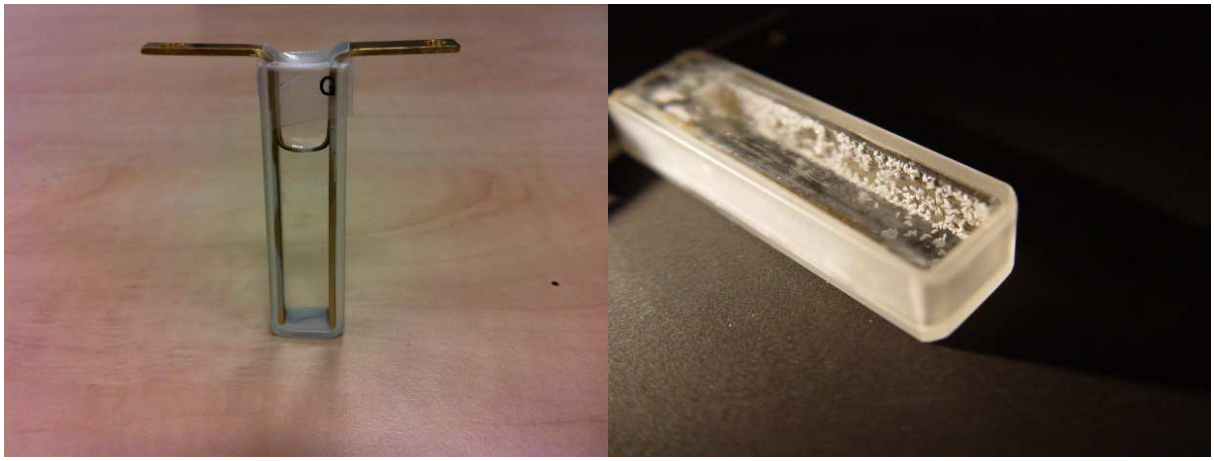

**Figure 32: The parallel-plate setup from up-close and the right photograph shows the crystal formation on the electrodes.**

# Appendix E Solvent selection

In designing an optimized process it is essential to select the proper solvent. Solvent selection is based on interaction with the electric field. In order to reduce this interaction with the electric field the solvent needs to have a low dielectric constant and a low dipole moment. A low dielectric constant means that higher electric fields can be obtained within the system. This is necessary because the electric field strength used to induce nucleation or aligning molecules was in the range of $10^5$ – $10^7$ V $m^{-1}$. The solvent acts like a capacitor within the system and thereby lowering the electric field. Appendix B explains more on this topic. A low dipole moment is advantageous, because it means that the solvent structure remains unaltered. So possible solvents are preferably non-polar with a low dielectric constant. From practical reasons other properties such as viscosity, boiling temperature, melting temperature, and toxicity are also considered. Table 4 shows some possible solvents based on these criteria.

**Table 4: Possible solvents for crystallization in an static electric field.**

| Solvents | Density [g/cm$^3$] | Dipole Moment [D] | Dielectric constant | Viscosity [mPs] |
|---|---|---|---|---|
| | | **Polar Protic** | | |
| Ethanol | 0.789 | 1.69 | 24.3 | 1.08 |
| Aniline | 1.018 | 1.55 | 6.8 | 3.77 |
| Acetic Acid | 1.049 | 1.74 | 6.15 | 1.22 |
| | | **Polar Aprotic** | | |
| THF | 0.886 | 1.63 | 7.52 | 0.461 |
| Ethyl Acetate | 0.894 | 1.78 | 6.02 | 0.426 |
| Nitrobenzene | 1.199 | 4.3 | 34.8 | 1.823 |
| | | **Non-polar** | | |
| Hexane | 0.655 | 0 | 2.02 | 0.292 |
| Toluene | 0.863 | 0.36 | 2.38 | 0.552 |
| 1,4-Dioxane | 1.027 | 0.4 | 2.2 | 1.255 |

From this table it can be concluded that the non-polar solvents are favourable due to their low dielectric constant and dipole moment. Because both model compounds are slightly polar, the only possible solvent is 1,4-dioxane. Both hexane and toluene are extremely non-polar and therefore the model compounds will not dissolve in them. So 1,4-dioxane possesses a low dielectric constant (2.2) and a low dipole moment (0.4 D), which makes it an ideal candidate for this study.

# Appendix F Electric field strength present in parallel-plate setup

The electric field strength in the parallel-plate capacitor is assumed to be homogeneous and is given by the following relation

$$E = \frac{\Delta V}{C \cdot d}$$

where $\Delta V$ is the potential difference, $C$ is the capacitance, and $d$ is the distance between the electrodes. In the next table the electric field strength are presented for several potential differences. The actual distance in the parallel-plate capacitor was 8 mm. Electric field strength has units of V $m^{-1}$.

**Table 5: Electric field present in the parallel-plate capacitor (d = 8 mm) for different solvents.**

| Solvent | 5 kV | 7.5 kV | 10 kV |
|---|---|---|---|
| Vacuum or air | 6,250E+05 | 9,375E+05 | 1,250E+06 |
| Ethanol | 2,572E+04 | 3,858E+04 | 5,144E+04 |
| THF | 8,311E+04 | 1,247E+05 | 1,662E+05 |
| Nitrobenzene | 1,796E+04 | 2,694E+04 | 3,592E+04 |
| Toluene | 2,626E+05 | 3,939E+05 | 5,252E+05 |
| 1,4-Dioxane | 2,841E+05 | 4,261E+05 | 5,682E+05 |

So electric field strengths in the order of $10^5$ V $m^{-1}$ could be obtained.

# Appendix G Solid Raman spectra

Solid Raman spectra were recorded from crystals obtained at different concentrations in order to check if this had an influence on the polymorphic outcome. Results are given for recrystallized isonicotinamide crystals at concentrations of 17, 30 and 35 mg $mL^{-1}$ at a cooling rate of 0.3 °C $min^{-1}$. Only for the C = 17 mg $mL^{-1}$ experiment a cooling rate of 1 °C $min^{-1}$ was used, because at lower cooling rates the time it took for crystals to appear was too long. Note that at all spectra were obtained in the absence of an electric field and that experiments were performed in the Crystalline setup.

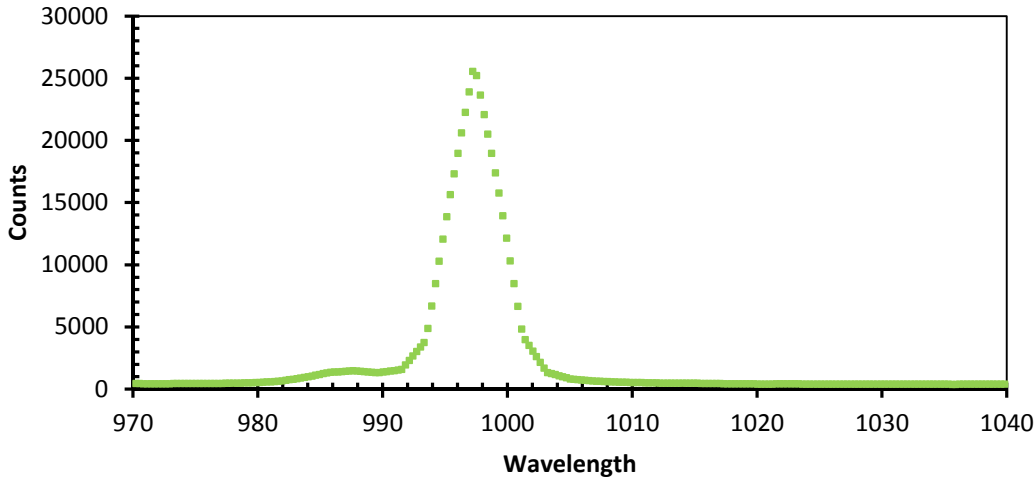


**Figure 33: Solid Raman spectra in the range of 970 and 1040 $cm^{-1}$ obtained from the recrystallized isonicotinamide crystals at C = 17 mg $mL^{-1}$. The characteristic peak lies at 998 $cm^{-1}$, which means that a metastable polymorph is obtained.**

This spectra is obtained at a recrystallization experiment at C = 17 mg $mL^{-1}$ and it can be seen that a metastable form is obtained.

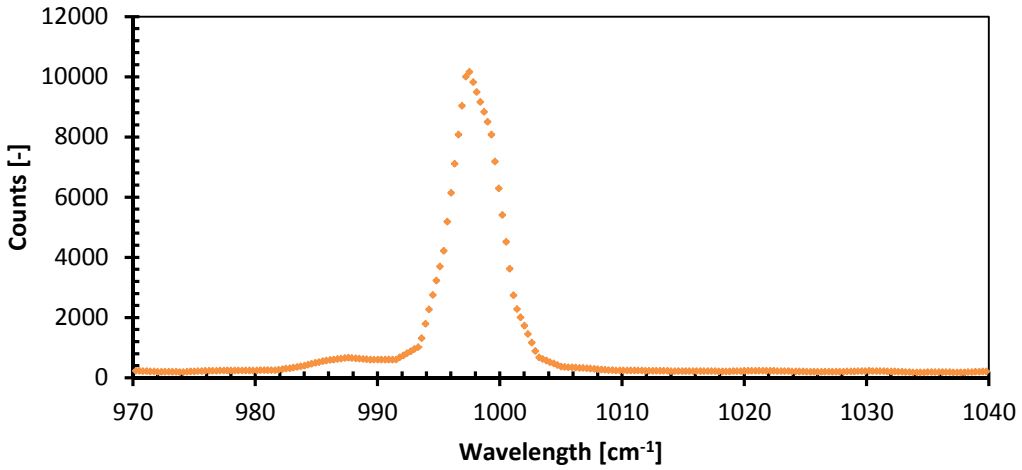


**Figure 34: Solid Raman spectra in the range of 970 and 1040 $cm^{-1}$ obtained from the recrystallized isonicotinamide crystals at C = 30 mg $mL^{-1}$. The characteristic peak lies at 998 $cm^{-1}$, which means that a metastable polymorph is obtained.**

This spectra is obtained at a recrystallization experiment at C = 30 mg $mL^{-1}$ and it can be seen that a metastable form is obtained.

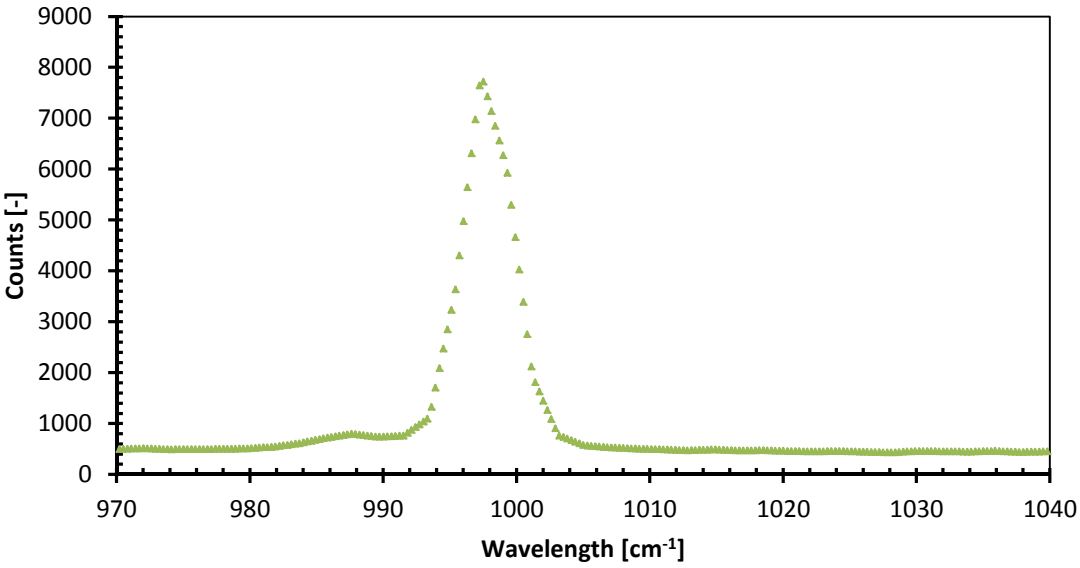


**Figure 35: Solid Raman spectra in the range of 970 and 1040 $cm^{-1}$ obtained from the recrystallized isonicotinamide crystals at C = 35 mg $mL^{-1}$. The characteristic peak lies at 998 $cm^{-1}$, which means that a metastable polymorph is obtained.**

This spectra is obtained at a recrystallization experiment at C = 35 mg $mL^{-1}$ and it can be seen that a metastable form is obtained. One can conclude that for this polymorphic system (isonicotinamide solved in 1,4-dioxane) the concentration has no effect on the crystal structure or polymorphic outcome of the cooling crystallization process.

Solid Raman spectra were recorded from crystals obtained at different cooling rates in order to check if this had an influence on the polymorphic outcome. Below the results for recrystallized isonicotinamide crystals (C = 35 mg $mL^{-1}$) are given for the cooling rates 0.1 and 0.3 °C $min^{-1}$. Note that at all spectra were obtained in the absence of an electric field and that experiments were performed in the Crystalline setup.

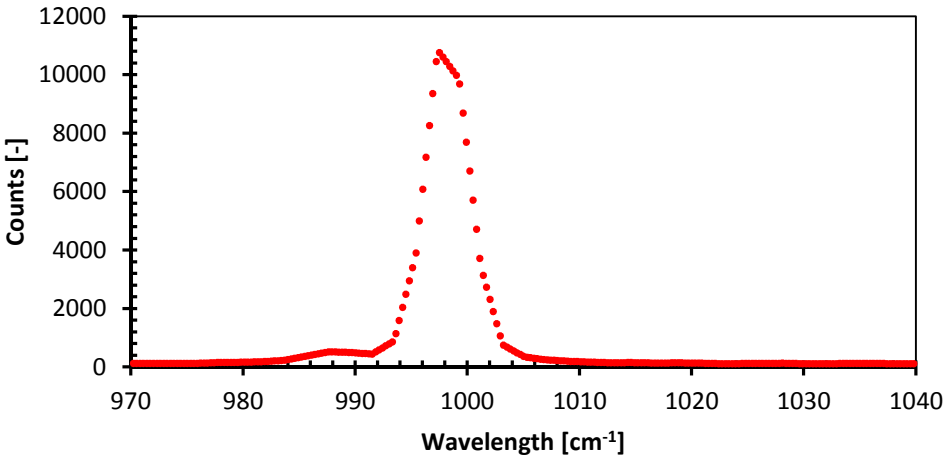


**Figure 36: Solid Raman spectra in the range of 970 and 1040 $cm^{-1}$ obtained from the recrystallized isonicotinamide crystals at 0.1 °C $min^{-1}$. The characteristic peak lies at 998 $cm^{-1}$, which means that a metastable polymorph is obtained.**

This spectra is obtained at a recrystallization experiment at C = 35 mg $mL^{-1}$, at a cooling rate of 0.1 °C $min^{-1}$ and it can be seen that a metastable form is obtained.

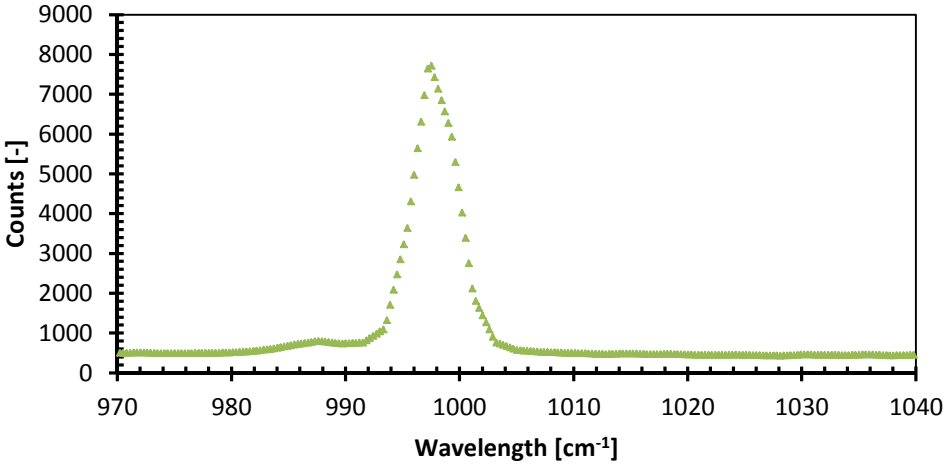


**Figure 37: Solid Raman spectra in the range of 970 and 1040 $cm^{-1}$ obtained from the recrystallized isonicotinamide crystals at 0.1 °C $min^{-1}$. The characteristic peak lies at 998 $cm^{-1}$, which means that a metastable polymorph is obtained.**

This spectra is obtained at a recrystallization experiment at C = 35 mg $mL^{-1}$, at a cooling rate of 0.3 °C $min^{-1}$ and it can be seen that a metastable form is obtained. These slow cooling rates are chosen, because it was investigated if the stable polymorph could be obtained from simple recrystallization experiments. At higher cooling rates the driving force is larger and so the chance of obtaining a stable form is less. But as one can see from the solid Raman spectra it seems that even at low cooling rates a metastable form is obtained.

Solid Raman spectra were recorded from crystals obtained from the anode and cathode in order to see if the obtained crystals were different on the separate electrodes. Below the results for recrystallized isonicotinamide crystals at C = 35 mg $mL^{-1}$, at cooling rate of 0.5 °C $min^{-1}$, and in the presence of a potential difference of +7.5 kV are given.

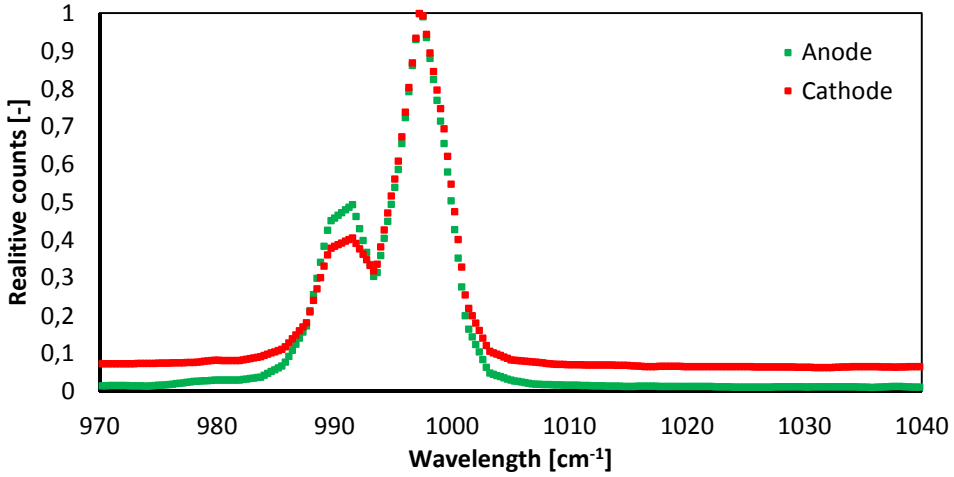


**Figure 38: Solid Raman spectra in the range of 970 and 1040 $cm^{-1}$ obtained from the recrystallized isonicotinamide crystals at the anode (green line) and cathode (red line) in the presence of the electric field.**

From the spectra it can be seen that the acquired crystals show no difference, so the electrodes do not have an influence on the polymorphic outcome.

The next spectra gives the difference between solid isonicotinamide crystals and dissolved isonicotinamide crystals in 1,4-dioxane.

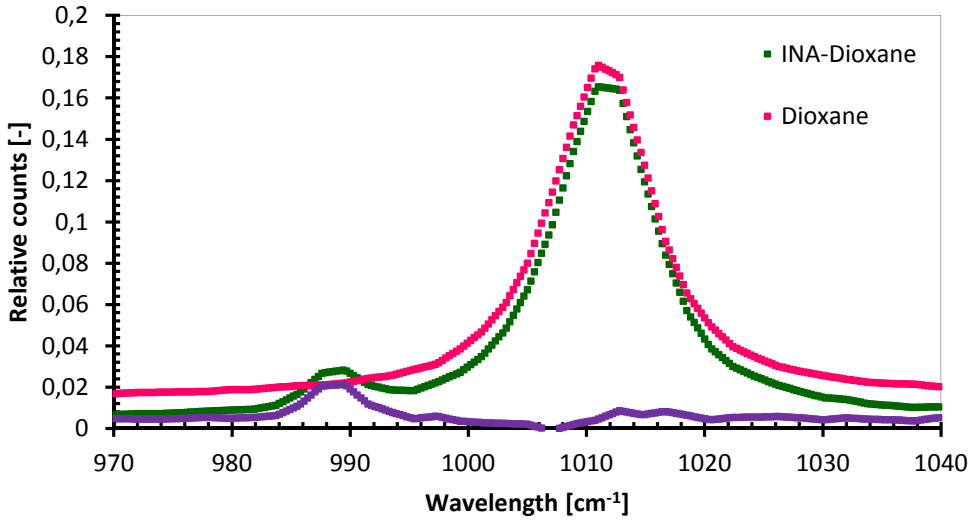


**Figure 39: Solid Raman spectra displaying the difference between INA crystals and INA crystals solved in 1,4-dioxane.**

The pink line gives the spectra of pure 1,4-Dioxane and the green line of isonicotinamide crystals in solution. One can see the characteristic peak of 1,4-dioxane at 1011 $cm^{-1}$ and for isonicotinamide at 990 $cm^{-1}$. The purple line gives the spectra of isonicotinamide crystals.

# Appendix H X-ray powder diffraction

This appendix gives the x-ray powder diffraction patterns of the acquired crystals of isonicotinamide and 4-hydroxybenzoic acid. Figure 40 depicts the XRPD patterns of all polymorphs of isonicotinamide and from the purchased isonicotinamide (dark blue line). It can be seen that the purchased material is indeed the stable polymorph (Form II).

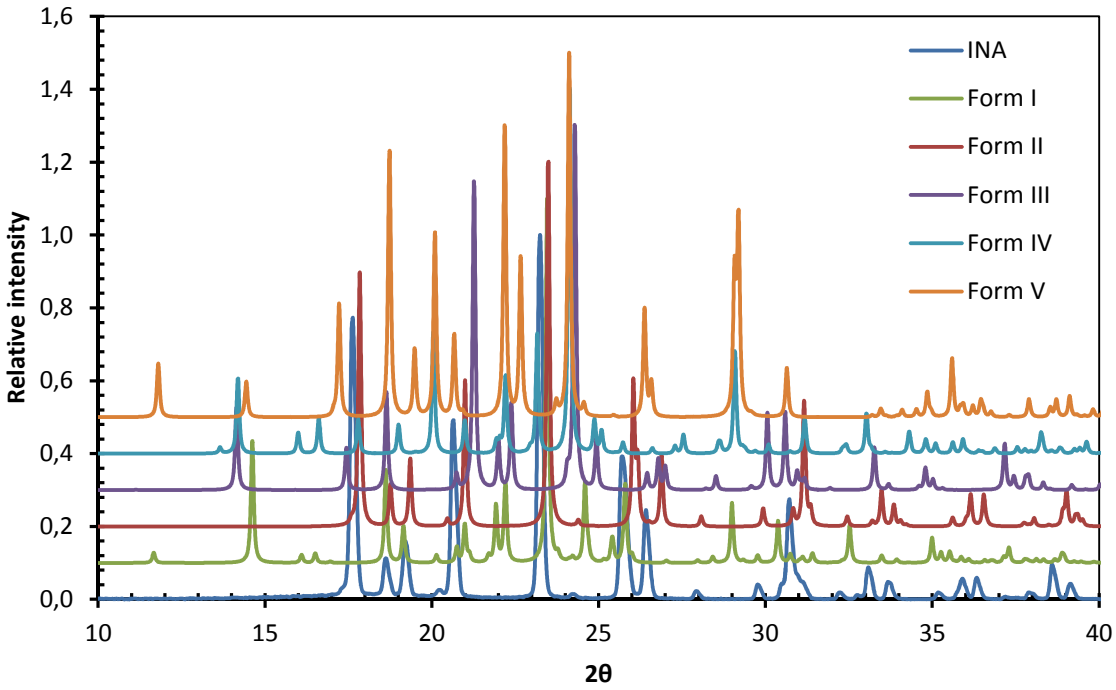


**Figure 40: X-ray powder diffraction patterns of all polymorphic forms of isonicotinamide. The stable polymorph is form II, whereas all other forms are metastable.**

The spectra of the isonicotinamide polymorphs were obtained from the Cambridge structural database (CSD). All the obtained patterns were compared to these database patterns and it was concluded that in the Crystalline experiments the polymorphic Form I (metastable) was obtained and in the parallel-plate setup polymorphic Form III (metastable) was obtained.

Next the XRPD patterns are given for the purchased isonicotinamide (blue line), the recrystallized material in the absence of the electric field (red line) and in the presence of the electric field (green line). The pattern of the purchased material shows that it was the stable form II, the recrystallized material in the absence of the electric field shows the pattern of form I and the recrystallized material in the presence of the electric field shows a mixture of the stable form II and form I. These results confirm what is seen with the solid Raman experiments.

Finally, the XRPD patterns for 4-hydroxybenzoic acid are given. The pattern of the purchased material (blue line), the recrystallized material in the absence of the electric field (red line) and in the presence of the electric field (green line) are given in figure 42. From this figure it can be seen that the pattern of the purchased material shows the stable form, the material recrystallized in the absence of the electric field produced a mixture of both polymorphs, and the material recrystallized in the presence of the electric field shows the metastable form. These results confirm what is seen with the solid Raman experiments.

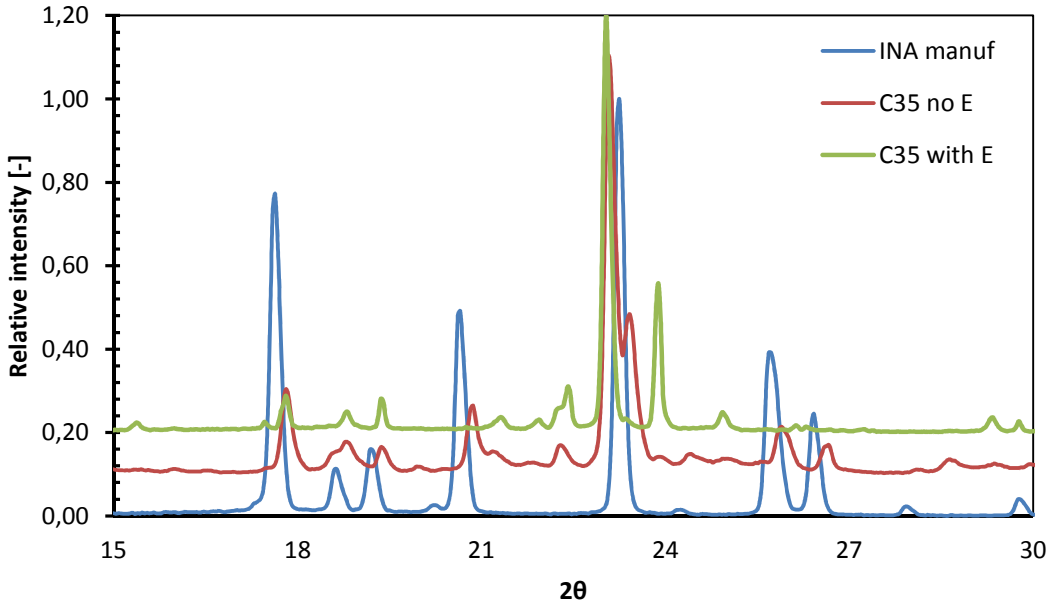


Figure 41: X-ray powder diffraction patterns of purchased isonicotinamide (blue line), recrystallized in the absence of an electric field (red line), and in the presence of an electric field (green line).

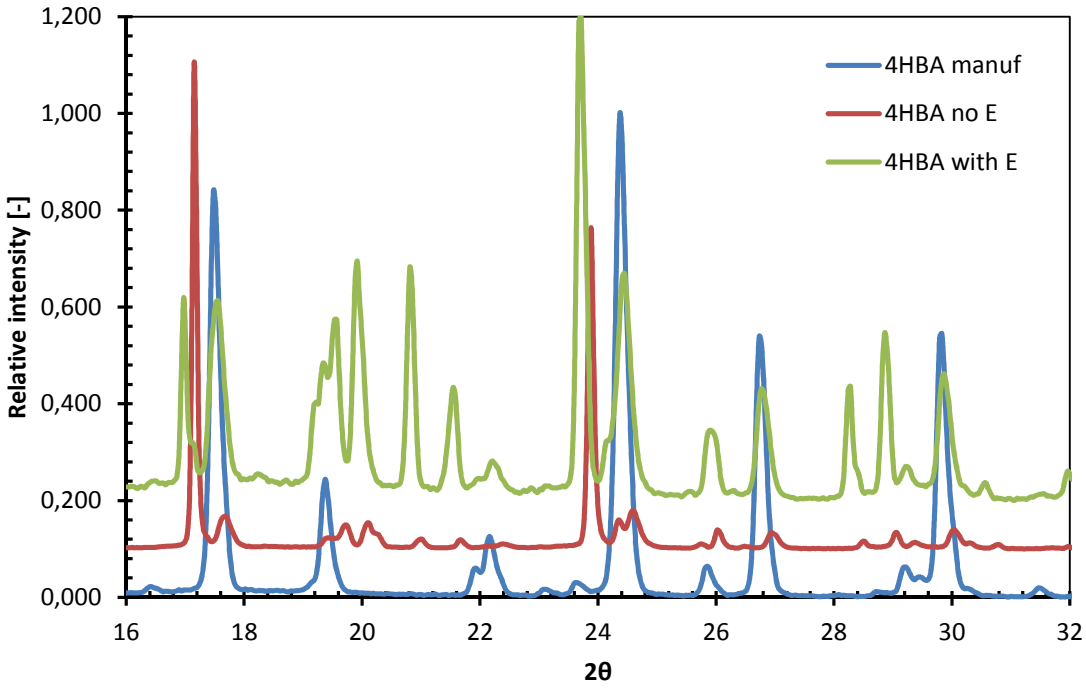


Figure 42: X-ray powder diffraction patterns of purchased 4-hydroxy benzoic acid (blue line), recrystallized in the absence of an electric field (red line), and in the presence of an electric field (green line).

# Appendix I Thermogravimetric analysis

Thermogravimetric analysis (TGA) is a thermal analysis technique used to characterize a wide variety of materials. TGA provides complimentary and supplementary characterization information to the most commonly used technique, which is differential scanning calorimetry (DSC). TGA measures the amount and rate of change as a function of temperature or time in a controlled atmosphere. The measurements are used primarily to determine the thermal and oxidative stabilities of materials as well as their compositional properties. The technique can analyze materials that exhibit mass loss (or gain) due to decomposition, oxidation or loss of volatiles.

Figure 43 shows the TGA (TGA 7, Perkin Elemer) results generated for two INA samples. The plot displays the percentage of mass as a function of sample temperature for the INA under a nitrogen purge. A 10 mg sample of INA recrystallized in Crystalline from a C = 30 mg $mL^{-1}$ (cooling rate of 0.1 °C $min^{-1}$) solution (1,4-dioxane) was heated at a rate of 10 °C $min^{-1}$ in a nitrogen atmosphere with a purge rate of 20 mL $min^{-1}$. The temperature program heated the sample from room temperature to 300 °C. The same experiment was conducted for an INA sample recrystallized from a C = 35 mg $mL^{-1}$ solution. TGA results show that INA undergoes thermal degradation beginning at $T_0$ = 185 °C with a total mass loss of 94.3%. There is a small amount (5.7%) of inert residue remaining. The extrapolated onset temperature ($T_0$) is used, because it is a reproducible temperature calculation and it is specified to be used by ASTM® and ISO.

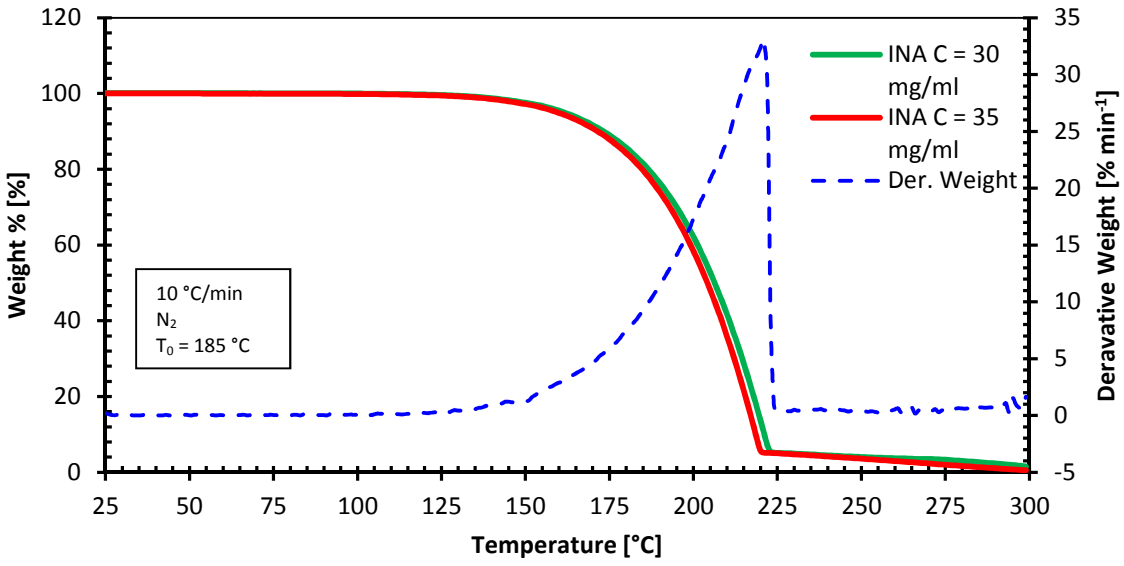


Figure 43: TGA of two samples of INA.

Moreover, from figure 43 it can be seen that the initial weight loss starts at 150°C and that the decomposition is finished at 220 °C. The original idea for using TGA was to check if the crystals formed a solvate with 1,4-dioxane. The boiling point of 1,4-dioxane is 101 °C and because there is no weight loss around this temperature one can conclude that no solvate is formed. Another observation is that the crystals obtained at both concentrations follow nearly the same temperature profile. The blue line indicates the derivative weight loss per minute, which shows how fast the decomposition takes place. So one can see at what temperature the decomposition rate was highest.

# Appendix J Induction time analysis

Induction times are obtained for three distinct concentrations (25, 30, 35 mg $mL^{-1}$). Experiments were performed in duplo for C = 25 and C = 35 mg $mL^{-1}$, because not all samples crystallized in time or they crystallized too soon to measure it accurately. In the first induction time experiment 52 out of the 128 samples crystallized. This low crystallization percentage is due to a low supersaturation ratio and thus a small driving force. These experiments took place in the metastable region in which no spontaneous nucleation occurs. The induction times obtained in the first crystallization experiment are depicted in figure 44.

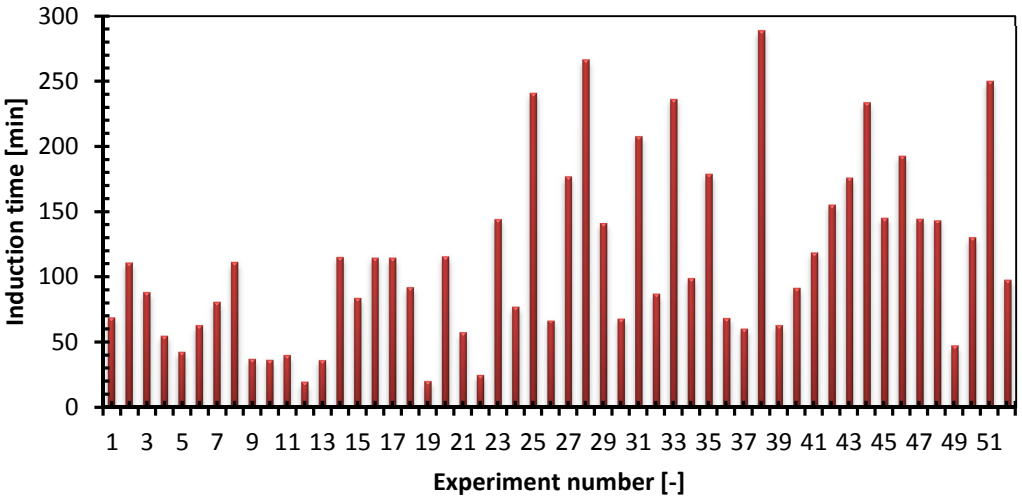


Figure 44: Induction times obtained at a concentration of 25 mg $mL^{-1}$. Experiments were done in the metastable zone.

In the second induction time experiment 61 out of the 64 samples crystallized. This crystallization percentage is due to a sufficient supersaturation ratio and thus a sufficient driving force. These experiments took place exactly on the metastable zone line. The induction times obtained in the second crystallization experiment are depicted in figure 45.

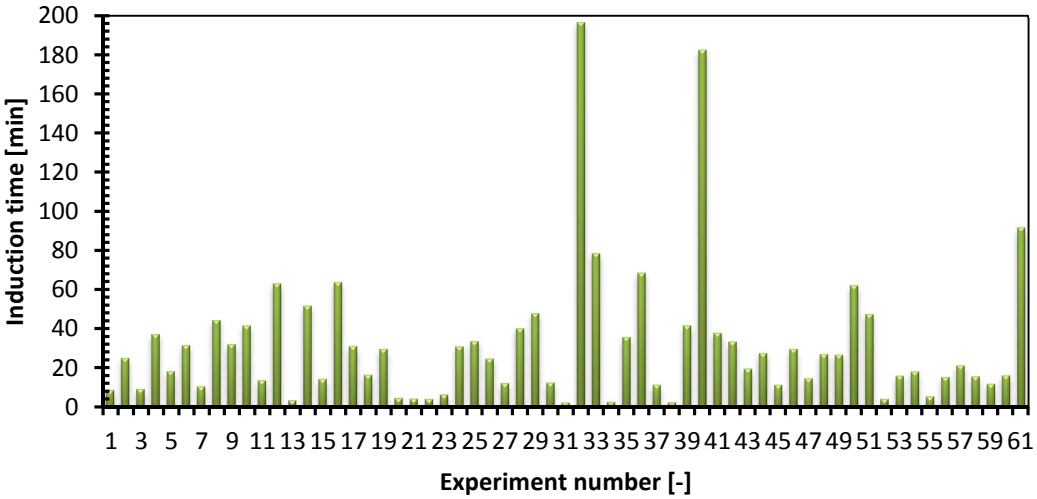


Figure 45: Induction times obtained at a concentration of 30 mg $mL^{-1}$. Experiments were performed on metastable line.

In the third induction time experiment 104 out of the 128 samples crystallized. This crystallization percentage is due to a high supersaturation ratio and thus a high driving force. Some of the samples crystallized so fast that an accurate measurement was not possible. These experiments took place above the metastable zone line in the spontaneous nucleation zone. The induction times obtained in the second crystallization experiment are depicted in figure 46.

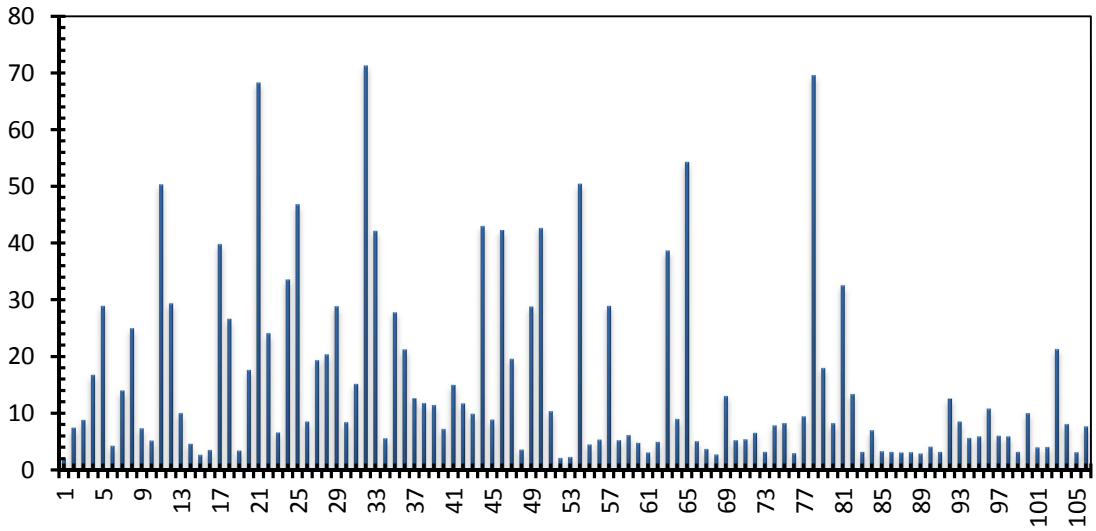


**Figure 46: Induction times obtained at a concentration of 35 mg $mL^{-1}$. Experiments were performed in the spontaneous nucleation region.**

Induction time is the period of time between the achievement of supersaturation and the detection of crystals. The induction times were measured at 25 °C.

# Appendix K Micrographs of INA crystals

This appendix shows the different crystals obtained from experiments with and without the electric field present. The experiments were performed in the parallel-plate setup with a concentration of 35 mg $mL^{-1}$, no agitation, and was air cooled. The micrographs depict crystals obtained from a cooling crystallization experiment where no electric field was present (0 V; top) and where the electric field was present (5 kV; middle and 10 kV; bottom)

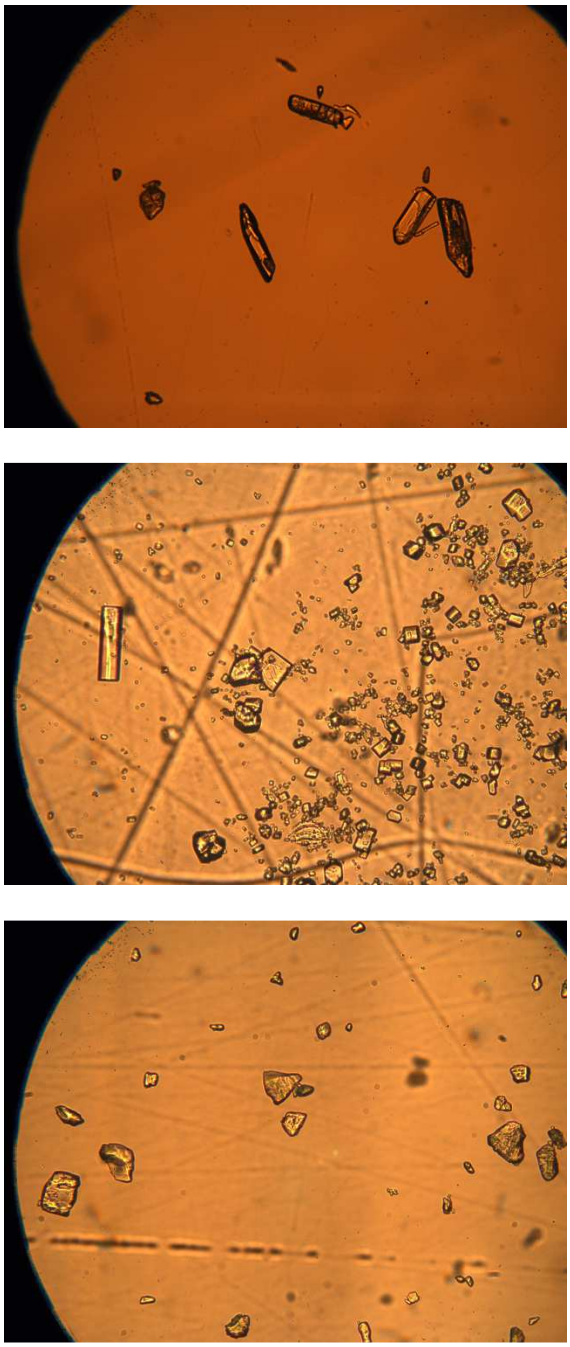

**Figure 47: Micrographs obtained from cooling crystallization experiment in the parallel-plate setup. Top: 0 kV; Middle: 5 kV; Bottom: 10 kV. Concentration was 35 mg $mL^{-1}$. All micrographs had magnification of 10x.**